The Astrophysical Journal, 720:581–602, 2010 September 1 doi:10.1088/0004-637X/720/1/581

SPECTROSCOPIC ANALYSIS OF HOT, HYDROGEN-RICH WHITE DWARFS: THE PRESENCE OF METALS AND THE BALMER-LINE PROBLEM*

A. Gianninas[1,4], P. Bergeron[1], J. Dupuis[2], and M. T. Ruiz[3,4]
[1] Département de Physique, Université de Montréal, C.P. 6128, Succ. Centre-Ville, Montréal, Québec H3C 3J7, Canada; gianninas@astro.umontreal.ca, bergeron@astro.umontreal.ca
[2] Canadian Space Agency, 6767 Route de l'Aéroport, Longueuil, Québec J3Y 8Y9, Canada; jean.dupuis@asc-csa.gc.ca
[3] Departamento de Astronomía, Universidad de Chile, Casilla 36-D, Santiago, Chile; mtruiz@das.uchile.cl
Received 2010 May 3; accepted 2010 July 4; published 2010 August 12

ABSTRACT

We present an analysis of optical spectra for 29 DAO white dwarfs. First, we present our new up-to-date model atmosphere grids computed without the assumption of local thermodynamic equilibrium in which we have included carbon, nitrogen, and oxygen at solar abundances. We demonstrate that the addition of these metals in the model atmospheres is essential in overcoming the Balmer-line problem, which manifests itself as an inability to fit all the Balmer lines simultaneously with consistent atmospheric parameters. We then present the spectroscopic analysis of our sample of DAO white dwarfs for which we determine the effective temperature, surface gravity, and helium abundance. We also present 18 hot DA white dwarfs that also suffer from the Balmer-line problem. We analyze these stars with models analogous to those for the DAO white dwarfs save for the presence of helium. Systematic differences between our newly determined atmospheric parameters with respect to previous determinations are explored. Far-ultraviolet spectra from the *FUSE* archive are then examined to demonstrate that there exists a correlation between higher metallic abundances and instances of the Balmer-line problem. The implications of these findings for all hot, hydrogen-rich white dwarfs are discussed. Specifically, the possible evolutionary scenario for DAO white dwarfs is revised and post-extreme horizontal branch evolution is no longer needed to explain the evolution for the majority of the DAO stars. Finally, we discuss how the presence of metals might drive a weak stellar wind which in turn could explain the presence of helium in DAO white dwarfs.

Key words: stars: abundances – stars: atmospheres – stars: fundamental parameters – white dwarfs

Online-only material: color figures

1. INTRODUCTION

One of the great achievements in white dwarf research over the last 20 years has been the ability to accurately measure the atmospheric parameters of these stars by comparing the theoretical predictions of model atmosphere calculations to observations throughout the electromagnetic spectrum. In particular, the spectroscopic technique developed by Bergeron et al. (1992) for analyzing the hydrogen-line (DA) white dwarfs has become the standard method for measuring the effective temperature and surface gravity of these stars which represent 80% of the white dwarf population.

Over the last several years, we have been conducting a spectroscopic survey based largely on the catalog of McCook & Sion (1999) and focusing on all the DA white dwarfs brighter than $V = 17.5$. High signal-to-noise ratio (S/N > 50) optical spectra for over 1300 white dwarfs have been secured and a preliminary analysis is presented in Gianninas et al. (2009). Of particular interest in this paper is that our sample includes a number of DAO white dwarfs. These are hot white dwarfs ($T_{\rm eff}$ > 40,000 K) that are characterized by optical spectra that exhibit absorption lines due to helium present in the atmosphere. Specifically, most DAO white dwarfs are distinguished by the He II λ4686 absorption feature in addition to the hydrogen Balmer lines. Since these stars clearly contain more than just hydrogen in their atmospheres, they need to be analyzed separately from the rest of our sample and require models which differ from our pure hydrogen models in order to properly measure their atmospheric parameters. We believe that this presents an opportunity to revisit in detail the DAO phenomenon and the connection with their hot DA counterparts.

Bergeron et al. (1994) presented an overview of the history and status of research on hot DA and DAO stars prior to their work. For the benefit of the reader, we provide a brief summary of that overview here. Initially, hot white dwarfs were expected to be sources of soft X-rays and extreme ultraviolet (EUV) radiation (Shipman 1976), but *Einstein* and *EXOSAT* data revealed instead that most hot DA stars had an X-ray flux deficiency (Vennes et al. 1988). It was thought that the presence of helium could explain the flux deficiency but Vennes et al. (1988) showed that radiation pressure could not support sufficient amounts of helium in the atmosphere to provide the necessary opacity. As an alternative, Vennes et al. (1988) proposed a model where a thin hydrogen layer floated in diffusive equilibrium above a more massive helium layer. These stratified models reproduced the X-ray and EUV data rather well (Koester 1989; Vennes & Fontaine 1992). Unfortunately, the survey conducted with *ROSAT* (Pounds et al. 1993) detected only 119 sources out of an expected 1000–2000 white dwarfs (Barstow 1989). Barstow et al. (1993) showed that neither homogeneous nor stratified models could explain these observations and they suggested that an additional opacity source, most likely metals, would provide a better match to the data.

The launch of the *Extreme Ultraviolet Explorer* (*EUVE*) and the spectroscopic data that it gathered permitted a more detailed

* Based on observations made with ESO Telescopes at the La Silla or Paranal Observatories under program ID 078.D-0824(A).
[4] Visiting astronomers at Las Campanas Observatory operated by Carnegie Institution of Washington.

study of the EUV flux of hot DA white dwarfs than the previous photometric surveys could. Analyses of the *EUVE* spectra showed that stratified atmospheres could not reproduce the data nearly as well as models that included metals (Barstow et al. 1997; Wolff et al. 1998). More sophisticated models that included the diffusion of the various metals through the atmosphere, in a self-consistent way, were subsequently computed and these matched the *EUVE* data even better (Dreizler & Wolff 1999; Schuh et al. 2002). As such, the notion that the flux deficiency in hot DA stars could be explained by stratified atmospheres, composed only of hydrogen and helium, was abandoned.

DAO white dwarfs, on the other hand, presented a different challenge since they clearly contained a much higher abundance of helium as evidenced by the appearance of the He II λ4686 absorption line in their optical spectra. It was possible that at least for this subgroup of white dwarfs the stratified atmospheres proposed by Vennes et al. (1988) might yet be valid. Indeed, DAO white dwarfs were unique in that their hybrid spectra provided a diagnostic tool by which the abundance and distribution of helium in the atmosphere could be studied directly.

The prototype of the DAO class, HZ 34, was identified as such by Wesemael et al. (1985) who presented the first spectroscopic analysis of DAO white dwarfs using homogeneous model atmospheres. Holberg (1987) significantly increased the number of known DAO stars and Holberg et al. (1989) combined optical and *International Ultraviolet Explorer* (*IUE*) observations to determine the atmospheric parameters of these stars. At the same time, Fontaine & Wesemael (1987) discussed the idea that most white dwarfs possibly descended from helium-rich PG 1159 stars. However, several studies had begun to show that several old planetary nebulae nuclei have hydrogen-rich atmospheres (Napiwotzki & Schönberner 1993). DAO white dwarfs might then represent a transition between the PG 1159 stars where hydrogen is diffusing upward to eventually form a hydrogen-rich layer at the surface. If that scenario were to be true, the stratified atmospheres of Vennes et al. (1988) would be the only viable models. However, a comprehensive analysis comparing the predictions of homogeneous and stratified model atmospheres to observations had never been conducted. It is for this reason that the study of Bergeron et al. (1994) is of particular importance as they were the first to perform a detailed analysis comparing optical and UV spectra to the predictions of both homogeneous and stratified atmospheres. Although their analysis of the UV spectra ultimately proved inconclusive, the He II λ4686 line profiles clearly pointed to homogeneous models as the stratified atmospheres produced line cores that were too shallow. Indeed all of the DAO white dwarfs in their sample were best reproduced with the homogeneous models, with the exception of PG 1305−017. As a consequence of this result, all subsequent analyses of DAO stars have employed homogeneous model atmospheres.

In addition to DAO white dwarfs, Bergeron et al. (1994) also looked at a number of hot DA stars. In particular, they explored the effects that trace amounts of helium (number ratios in the range $\mathrm{He/H} = 10^{-5}$ to 10^{-4}) would have on the atmospheric parameter determinations. They found significant differences between the pure hydrogen models and those including helium. However, it was later shown by Napiwotzki (1997) that this was due to the fact that Bergeron et al. (1994) computed models assuming local thermodynamic equilibrium (LTE) since the effects due to the presence of helium vanish when models are computed assuming non-LTE (NLTE) conditions. It should also be noted that the stratified models were also computed in LTE, and NLTE versions of those models, and the subsequent helium line profiles associated with them, have never been explored.

Another important result from that study was the realization that most of the DAO stars in their sample were afflicted with the so-called Balmer-line problem. This problem manifests itself as an inability to simultaneously fit all the Balmer lines with consistent values of $T_{\rm eff}$ and $\log g$, and it was first observed by Napiwotzki (1992, 1993) in his analysis of central stars of planetary nebulae (hereafter, CSPNe). More specifically, the line profiles of Hβ, and to a lesser extent Hγ, are predicted too shallow and thus require a lower temperature to correctly fit the observations. It should be noted that the Balmer-line problem was not observed in any of the hot DA stars analyzed by Bergeron et al. (1994). This would suggest that the mechanism responsible for the Balmer-line problem was operating only in DAO stars. Consequently, several solutions to this problem were explored. Bergeron et al. (1993) included blanketing due to iron in their model atmospheres in an effort to fit the line profiles of Feige 55. Although they were successful, they used an iron abundance of $\log \mathrm{Fe/H} = -3.0$ which is unrealistically high (15 times solar) and their models were computed assuming LTE conditions. Furthermore, Napiwotzki & Rauch (1994) reviewed several failed explanations to the Balmer-line problem such as magnetic fields, wind effects, and pressure ionization. They also explored another possibility by looking at ion-dynamical effects on the Stark broadening of hydrogen lines, but this also proved unsuccessful.

A solution to the Balmer-line problem was eventually achieved and presented by Werner (1996). His solution was to include carbon, nitrogen, and oxygen (hereafter, CNO) at solar abundances in the calculation of the model atmosphere. Although such calculations had already been performed in the past (Werner & Heber 1991; Werner & Dreizler 1993), Werner (1996) showed that the decisive ingredient was the necessity to include the proper Stark broadening of the metallic lines. The net effect was a cooling of the upper layers of the atmosphere where the core of the Balmer lines is formed. In this temperature regime, cooler temperatures translate to deeper line cores. As such, these new models were in very good agreement with the observed line profiles.

Other important studies of hot DAO white dwarfs since then have come from Napiwotzki (1999) who analyzed a large sample of CSPN, 15 of which turned out to be DAO white dwarfs. Interestingly, Napiwotzki (1999) did not implement the solution to the Balmer-line problem outlined by Werner (1996). Instead, he relied on the fits of the higher Balmer lines, namely Hδ and Hϵ, which are formed deeper in the atmosphere where the thermodynamic structure is not affected by the presence of CNO. The reasons for omitting the solution are twofold. First, Napiwotzki (1999) argued that CNO abundances would need to be known for each star and that the computational time required to include CNO in NLTE models was too great.

More recently, far-ultraviolet (FUV) spectra of DAO white dwarfs obtained with the *Far-Ultraviolet Spectroscopic Explorer* (*FUSE*) were analyzed in a series of papers by Good et al. First, Good et al. (2004) wanted to verify if consistent temperatures can be obtained by independently fitting the Balmer lines in the optical spectrum and the Lyman lines in the FUV spectrum. Instead, they observed a similar trend to the one highlighted by Barstow et al. (2003) with the Lyman lines systematically yielding higher temperatures as compared with those derived from the Balmer lines. It should be noted that the NLTE model

atmospheres used by Good et al. (2004) in their analysis did include CNO as prescribed by Werner (1996). Second, Good et al. (2005a) exploited the time-resolved nature of *FUSE* data to check for binarity among DAO white dwarfs. They did not detect evidence for any new binaries but their technique did detect radial velocity variability for all the known binaries in their sample. Finally, Good et al. (2005b) obtained abundance measurements for the various metals whose absorption lines abound in the FUV of these DAO white dwarfs. However, due to the difficulties of computing a full grid of models to measure, in an absolute manner, the abundances of all the observed species (C, N, O, Si, Fe, and Ni), the abundance determinations are measured relative to the measured abundances in G191-B2B (Barstow et al. 2001b).

Finally, one of the biggest developments in recent times in the white dwarf community has been the wealth of observational data produced by the Sloan Digital Sky Survey (SDSS). Having now surpassed the 10,000 mark in terms of newly discovered white dwarf stars, it should come as no surprise that new DAO white dwarfs are among them. Hügelmeyer et al. (2007) present an analysis for 16 new DAO white dwarfs discovered in the SDSS up to and including Data Release 4 (Eisenstein et al. 2006). Unfortunately, as is often the case, many of the spectra lack the S/N necessary in order to accurately measure their atmospheric parameters (Gianninas et al. 2005, Section 2.1). Furthermore, Hügelmeyer et al. (2007) use H/He model atmospheres that do not include CNO to deal with the Balmer-line problem. In addition, they do not restrict their analysis to the higher Balmer lines like Napiwotzki (1999) did, instead they include both Hβ and Hγ in their fits thus increasing the uncertainty of their measured atmospheric parameters.

We believe that the time is right to take a fresh look at the DAO phenomenon using high S/N spectra coupled with model atmospheres that take into account all that we have learned about these stars over the past 15 years. In addition, and similarly to Bergeron et al. (1994), we also include an analysis of hot DA white dwarfs found in the same range of effective temperature as the DAO stars. Indeed, we will see that several distinct groups of objects emerge from this analysis and that DAO and hot DA stars have more in common than we might have been led to believe in the past. We present in Section 2 our spectroscopic observations and in Section 3 we describe the various grids of model atmospheres and synthetic spectra that we computed for our analysis. The results from our analysis of optical spectra are presented in Section 4. In Section 5, we examine the *FUSE* data for our ensemble of white dwarfs. In Section 6, we discuss the implications of our findings and finally, we make some concluding remarks in Section 7.

2. SPECTROSCOPIC OBSERVATIONS

Our optical data are taken from the ongoing spectroscopic survey of DA white dwarfs outlined in Gianninas et al. (2009). Since we are interested in the temperature range where DAO stars are found, we restrict ourselves to stars with $T_{\rm eff} > 40{,}000$ K. This translates to a total of 152 white dwarfs of which 29 are DAO white dwarfs. However, the spectrum we obtained for 0625−253 was completely dominated by the emission lines of the associated planetary nebula (A15) and so we were forced to drop this object from our sample. The spectra of the 29 DAO white dwarfs come from several sources. First of all, there are 12 stars for which the spectra are identical to those used by Bergeron et al. (1994) in their analysis. Of the remaining 17 spectra, 13 have been obtained as part of our ongoing spectroscopic survey (Gianninas et al. 2009). This includes new spectra of Feige 55 (1202+608) and PG 1210+533, both of which are white dwarfs analyzed in Bergeron et al. (1994). With the exception of five spectra (Feige 55, 0458−303, 0950+139, 1136+667, and 1958−501), all of our data were obtained at Steward Observatory's 2.3 m telescope equipped with the Boller & Chivens spectrograph. The 4.″5 slit together with the 600 line mm^{-1} grating blazed at 3568 Å in first order provides a spectral coverage from about 3000–5250 Å at a resolution of ∼6 Å (FWHM). The spectrum of Feige 55 was obtained at the 1.6 m telescope of the Observatoire du Mont-Mégantic where the 600 line mm^{-1} grating provided a spectral coverage from about 3100–7500 Å at a similar resolution. 0458−303 was observed at ESO's 3.6 m telescope at La Silla, Chile with the ESO Faint Object Spectrograph and Camera (v.2) (EFOSC2). The no. 7 grism and a 1.″0 slit provided a spectral coverage from about 3300–5200 Å with a resolution of ∼6 Å (FWHM). The spectrum of 0950+139 was obtained using the Mt. Hopkins 6.5 m MMT telescope using the Blue Channel of the MMT Spectrograph. The 500 lines mm^{-1} grating and a 1.″0 slit provided a spectral coverage from about 3400–6300 Å with a resolution of ∼4 Å (FWHM). 1136+667 is in a binary system with a K dwarf and the spectrum we obtained was heavily contaminated with emission lines to the point where our spectroscopic analysis technique was rendered useless. Luckily, this object had been previously studied by Sing et al. (2004). In their work, they obtained a spectrum at inferior conjunction (see their Figure 9) which is almost devoid of contamination and which they kindly provided to us. Finally, the spectrum of 1958−501 was obtained at Carnegie Observatories' 2.5 m Irénée du Pont Telescope at Las Campanas, Chile with the Boller & Chivens spectrograph. The 1.″5 slit with the 600 line mm^{-1} grating blazed at 5000 Å provided a spectral coverage from about 3500–6600 Å at a slightly better resolution of ∼3 Å (FWHM).

Of these 29 white dwarfs, 26 have already been identified as being of the DAO spectral type. The remaining three (0458−303, 1201−049, and 1958−501) are identified as members of the DAO class for the first time in this paper. Finally, we wish to address the case of 2218+706. This star was classified as a DAO white dwarf by Barstow et al. (2003) based on their detection of a "trace" of He II λ1640 in the ultraviolet (Barstow et al. 2001a). This detection is not an especially strong indicator as He II λ1640 has only rarely been detected in DAO white dwarfs (Holberg et al. 1989; Bergeron et al. 1994). More importantly, white dwarfs are classified based on features observed in their *optical* spectra. In that respect, we concur with Barstow et al. (2003) as we detect no sign of He II λ4686 in our optical spectrum. However, if we consider the abundance of He/H = 3×10^{-5} determined by Barstow et al. (2001a), it would be impossible to detect any trace of He II λ4686 with our medium resolution spectrum. Therefore, for the purposes of our analysis, we will consider 2218+706 as a simple DA white dwarf.

The 29 spectra of our DAO white dwarfs are displayed in Figure 1. First of all, we note that all the spectra have a relatively high S/N with a minimum of S/N ∼ 50. Second, we see that all the spectra show, besides the hydrogen Balmer lines from Hβ to Hϵ, the He II λ4686 line signaling the presence of helium in the atmosphere (the weakness of the helium line observed in 1201−049 is further discussed in Section 6.1; see also Figure 21). However, this is not the only feature of note in the spectra of these DAO white dwarfs. Several spectra (0950+139

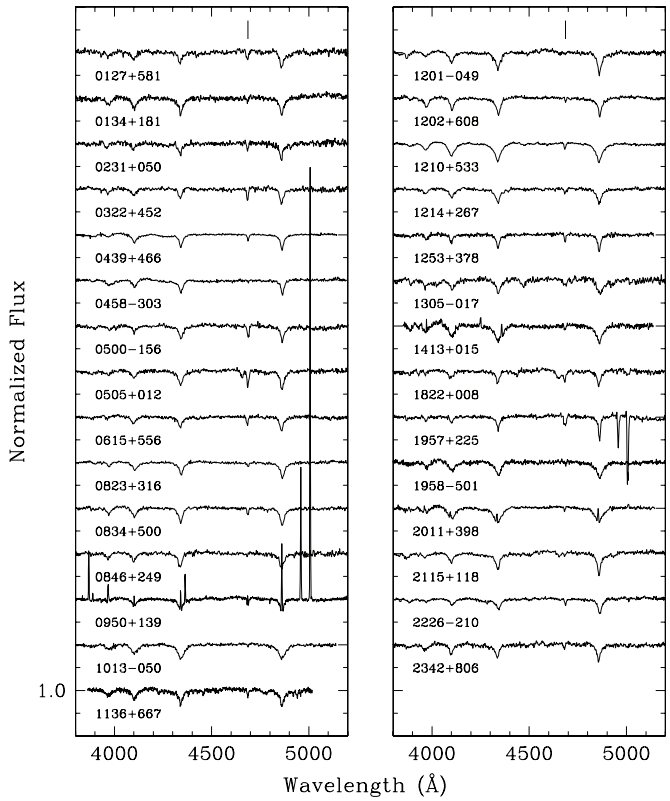

Figure 1. Optical spectra for the 29 DAO stars in our sample in order of increasing right ascension from top left to bottom right. The spectra have been normalized to a continuum set to unity and vertically shifted for clarity. The tick mark at the top of each panel indicates the location of the He II λ4686 absorption line.

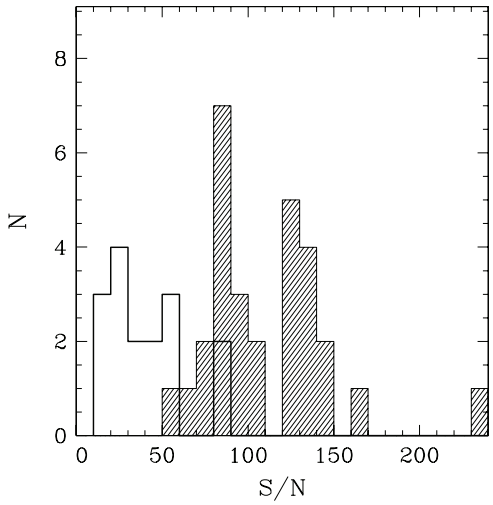

Figure 2. Distribution of S/N for our sample of 29 DAO white dwarfs (dashed histogram) and the 16 SDSS DAO white dwarfs from Hügelmeyer et al. (2007) (solid line histogram).

and 2011+398) also contain emission lines. In the case of 0950+139, these are due to the contribution of a planetary nebula still present around the star. On the other hand, the emission lines in 2011+398 are the result of this star being in a binary system with an M dwarf (Barstow et al. 1995). The contamination due to the emission lines varies from one spectrum to another and will complicate our analysis, especially in cases where there is emission in the core of the Balmer lines. In the case of 1957+225, emission lines from the accompanying planetary nebula were slightly oversubtracted during the removal of the background during data reduction and now appear as two deep and narrow absorption lines redward of Hβ. Furthermore, four of these stars (0505+012, 1201−049, 1822+008, and 2115+118) are actually of spectral type DAOZ due to the presence of metallic absorption lines in their spectra. Specifically, it is the C IV λ4658 line which is observed just blueward of He II λ4686 in all of these stars. 0505+012 was originally identified by Heber et al. (1996) whereas we classify 1201−049 as DAOZ for the first time in this work. 1822+008 was classified as both a DAOZ white dwarf and a PG 1159 star by Napiwotzki & Schönberner (1995). In the subsequent analyses of Dreizler et al. (1995b) and Napiwotzki (1999), the DAOZ classification was dropped altogether and 1822+008 was considered as a hybrid PG 1159 star due to the presence of strong Balmer lines. However, as we will see below, the atmospheric parameters we obtain for this star place it squarely in the realm of the DAO stars. Specifically, we obtain a lower $T_{\rm eff}$ and a higher log g value than Napiwotzki (1999, see his Table 1). As such, we believe that the initial classification of DAOZ is the correct one. Finally, Dreizler et al. (1995a) were the first to identify 2115+118 as being of the DAOZ spectral type. Indeed, in their spectrum of 2115+118 (see their Figure 1), they identify absorption lines due to highly ionized C, N, O, and even Ne.

Finally, we show in Figure 2 a comparison of the S/N of our sample of DAO stars with the SDSS DAO stars analyzed by Hügelmeyer et al. (2007). We see that *all* of the DAO white dwarfs from our sample have S/N greater than 50 whereas the peak of the SDSS distribution is near 20. We see once again the great weakness of the SDSS whose spectra have S/N too low to precisely measure the atmospheric parameters of these stars (Gianninas et al. 2005).

3. MODEL ATMOSPHERES AND SYNTHETIC SPECTRA

For the analysis of our sample of DAO white dwarfs, we have computed several new grids of model atmospheres and synthetic spectra that take into account advances (since Bergeron et al. 1994) in our knowledge and understanding of DAO white dwarfs as well as the physics and composition of their stellar atmospheres. In particular, we have computed separate grids assuming both LTE and NLTE as well as models containing CNO in order to study their effects on the thermodynamic structure of the atmosphere and how those changes translate to the theoretical Balmer-line profiles. Our models and synthetic spectra were all computed using the TLUSTY atmosphere code and the accompanying spectrum synthesis code SYNSPEC, both developed by Hubeny & Lanz (1995). All the model atmospheres are homogeneous in terms of their chemical composition (cf. Section 1).

As for the emergent spectra, we use the improved Stark profiles developed by Tremblay & Bergeron (2009) for our hydrogen line profiles, instead of the tables of Lemke (1997), and the calculations of Schöning & Butler (1989) for the profiles of He II λ1640 and λ4686. The implications of the improved hydrogen line profiles from Tremblay & Bergeron (2009) on our derived atmospheric parameters will be qualitatively discussed in Section 4.4. The atmospheric parameters cover a range of $T_{\rm eff}$ = 40,000 (5000) 90,000 K and $T_{\rm eff}$ = 90,000 (10,000) 150,000 K (where the quantity in parentheses indicates the step size), log g = 6.5 (0.5) 8.5 and log He/H = −5.0 (1.0) 0.0.

The first major change relative to the models used in the Bergeron et al. (1994) analysis is the computation of models

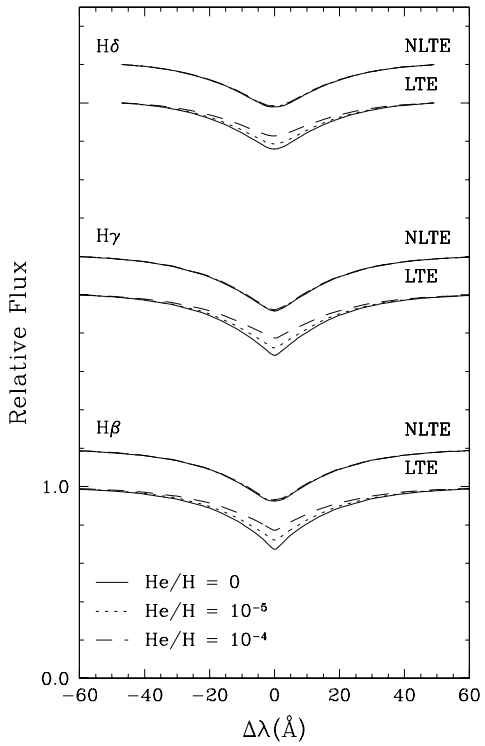

Figure 3. Normalized Balmer-line profiles for Hβ, Hγ, and Hδ computed for different helium abundances both in LTE and NLTE for a model atmosphere at $T_{\rm eff} = 65{,}000$ K and $\log g = 7.5$.

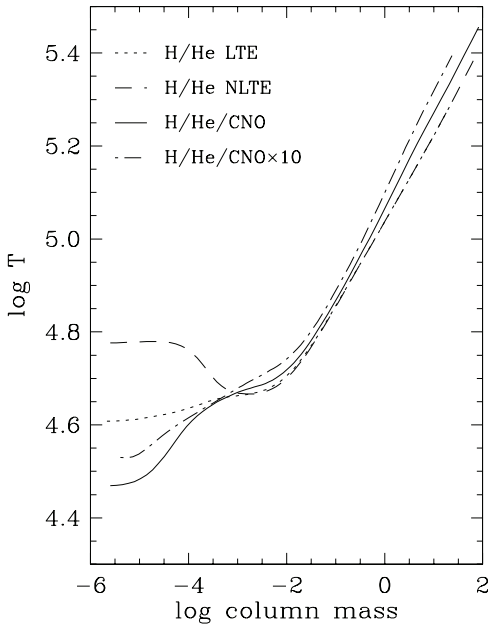

Figure 4. Temperature structure as a function of column mass for a reference model atmosphere at $T_{\rm eff} = 65{,}000$ K, $\log g = 7.5$, and $\log {\rm He/H} = -3.0$. The dotted line represents a model with H and He computed with the assumption of LTE whereas the dashed line was computed in NLTE. The solid line depicts a model with H, He, and CNO computed in NLTE. Finally, the dash-dotted line represents a model with H, He, and a CNO abundance enhanced by a factor of 10 and computed assuming NLTE.

in NLTE. The combination of modern computing power and the TLUSTY code makes it possible to compute NLTE models rather easily and within a reasonable time frame, a much more difficult task in the past. In particular, it is clear that NLTE effects are important in white dwarfs in this temperature range (Napiwotzki et al. 1999). DAO white dwarfs are particularly susceptible since they are all hot and generally have lower surface gravities than normal DA stars, which favors departures from LTE conditions. Bergeron et al. (1994) had demonstrated that traces of helium in hot DA stars had an effect on the Balmer-line profiles, and consequently on the atmospheric parameters measured for those stars. However, the models in Bergeron et al. (1994) were all computed assuming LTE conditions. Napiwotzki (1997) showed that when these same models are computed assuming NLTE, the presence of helium has no effect on the Balmer-line profiles. They concluded that for an LTE analysis of the Balmer lines, pure hydrogen models should be used even if traces of helium are present in the atmosphere. Consequently, for an analysis of the Balmer lines in DAO white dwarfs which, by definition, contain helium in the atmosphere, it is imperative to compute models in NLTE.

As a first test of our new models, we show in Figure 3 a comparison between line profiles computed in LTE and NLTE, and with varying traces of helium for a model atmosphere at $T_{\rm eff} = 65{,}000$ K, $\log g = 7.5$. We see that in the LTE case the presence of helium affects the line cores producing shallower lines as the helium abundance increases. In contrast, the line profiles computed in NLTE are identical regardless of the helium abundance and thus we are in perfect agreement with the results of Napiwotzki (1997). This result further reinforces the need to calculate NLTE atmospheres in order to properly model white dwarfs in this temperature regime, the more so that our technique for determining the atmospheric parameters for these stars rests on our ability to reproduce the Balmer-line profiles in detail.

Table 1
Ions Included in the Model Atmospheres

Ion	Levels	Super Levels	Transitions
C III	16	7	92
C IV	21	4	150
N III	25	7	184
N IV	15	8	97
N V	10	6	86
O III	20	9	141
O IV	31	8	270
O V	34	6	222
O VI	15	5	116

The second, and possibly more important difference with the previous generation of models, is the addition of CNO at solar abundances (as listed in Asplund et al. 2005) as the solution to the Balmer-line problem. Werner (1996) showed that the inclusion of these metals with the proper Stark broadening effectively solves the Balmer-line problem by cooling the upper layers of the atmosphere where the core of the lower Balmer lines are formed, most notably Hβ and to a lesser extent Hγ. The addition of these metals is further supported by the fact that they have since been detected in the UV spectra of many DAO white dwarfs and hot white dwarfs in general (Barstow et al. 2003; Good et al. 2005a). For completeness, we list in Table 1 all the ions of CNO included in our models along the with the number of super levels (as defined in Hubeny & Lanz 1995) and total transitions included for each ion. All the model atoms are taken from the TLUSTY Web site.[5]

To better illustrate the effects of the addition of CNO and the assumption of NLTE on the thermodynamic structure of the atmosphere, we show in Figure 4 the temperature structure for four reference model atmospheres computed at $T_{\rm eff} = 65{,}000$ K,

[5] http://nova.astro.umd.edu/Tlusty2002/tlusty-frames-data.html

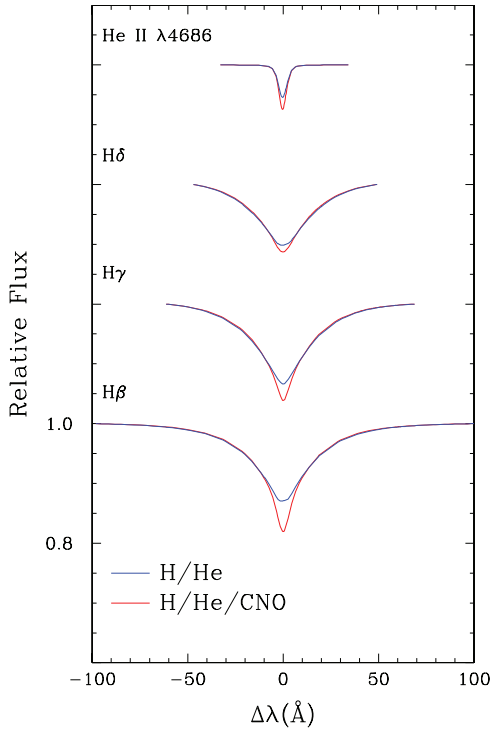

Figure 5. Normalized Balmer-line profiles for Hβ, Hγ, Hδ, and He II λ4686 computed in NLTE with (red) and without (blue) CNO for a model atmosphere at $T_{\rm eff} = 65{,}000$ K, $\log g = 7.5$, and $\log {\rm He/H} = -3.0$.

(A color version of this figure is available in the online journal.)

$\log g = 7.5$, and $\log {\rm He/H} = -3.0$. The first model is a model with H and He computed assuming LTE, the second is identical but computed in NLTE, and in the third we have the addition of CNO. The fourth model was computed with the CNO abundances enhanced by a factor of 10; this model will be discussed in greater detail later. We see that the NLTE effects actually cause the classical heating of the surface regions with respect to the LTE model. In contrast, the inclusion of CNO causes a cooling of the surface regions, even cooler than the LTE model. Let us now examine what effect these changes have on the Balmer-line profiles. In Figure 5, we compare Balmer-line profiles for two models, both computed in NLTE, one with CNO and one without. We see that the cooling effect of the CNO in the upper atmosphere produces line profiles with much deeper cores. The core of the Balmer lines is formed higher up in the atmosphere due to the higher opacity in the line center, and since the Balmer lines become deeper as temperature decreases in this temperature regime, we obtain line profiles with deeper cores, as required. Our results are thus in agreement with the results of Werner (1996) and we have essentially overcome the Balmer-line problem. As a test of this statement, we have attempted to reproduce in Figure 6 the analysis shown in Figure 3 of Werner (1996) for the same two stars, namely, BD+28 4211 and LS V+46 21 (0439+466). In both cases, we are not showing formal fits to the data but simply a superposition of the synthetic spectrum and the observed spectrum. In the case of LS V+46 21, we note the significant difference seen in the line cores, in particular for Hβ and Hγ. The models that include CNO allow for much deeper line cores, as previously stated, and thus reproduce the observed line profiles of LS V+46 21 quite well, as was the case for Werner (1996). We should note, however, that the effect of the CNO is exaggerated when comparing two models for a given set of atmospheric parameters. As we will

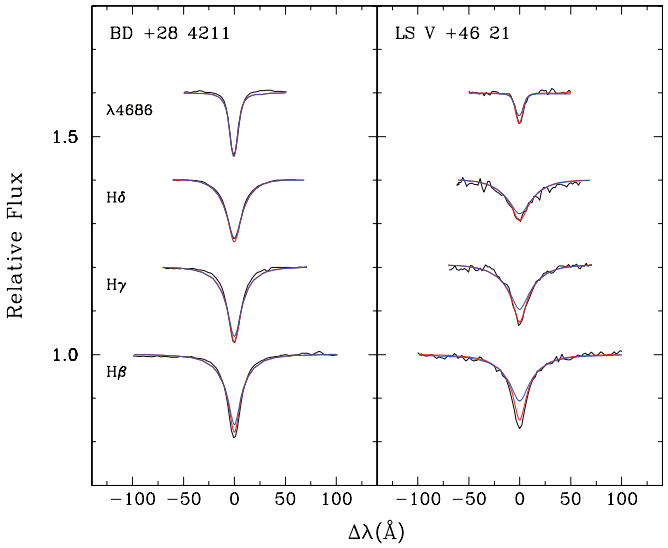

Figure 6. Comparison of the observed line profiles for BD+28 4211 and LS V+46 21 with synthetic spectra obtained from model atmospheres with (red) and without (blue) CNO.

(A color version of this figure is available in the online journal.)

see, the effect is less pronounced when comparing two fits of the same star since all three parameters ($T_{\rm eff}$, $\log g$, and $\log {\rm He/H}$) are allowed to vary to achieve the best possible match between the models and the data.

The case of BD+28 4211 is somewhat different. First of all, the parameters used by Werner (1996), $T_{\rm eff} = 82{,}000$ K, $\log g = 6.2$, and $\log {\rm He/H} = -1.0$, are based on an analysis of the Fe V/Fe VI ionization balance by Napiwotzki (1993). Neither Werner (1996) or Napiwotzki (1993) performed a formal fit to the observed line profiles of BD+28 4211 with an appropriate set of models. As such, our parameters ($T_{\rm eff} = 63{,}210$ K, $\log g = 6.57$, and $\log {\rm He/H} = -1.14$) differ significantly from those used by Werner (1996). Furthermore, we see that the effect of the CNO in the case of BD+28 4211 is much more subtle than what is seen in Werner (1996). This is because we are comparing H/He models in NLTE with similar models to which we have added CNO. In contrast, Werner (1996) compared H/He models computed with *Doppler* profiles to his final Stark broadened CNO models. In any case, the relevance of BD+28 4211 in this discussion is mitigated by the fact that it is not even a white dwarf, but rather a subdwarf O star.

As a final consistency check of our models, we have taken our reference model, which includes CNO, and have artificially added noise to the corresponding synthetic spectrum to simulate an S/N of 200. We then fitted this synthetic spectrum with our grid that does not contain any metals. Similarly, we created a synthetic spectrum based on our model with enhanced CNO abundance (CNO $\times$ 10) and fitted it with our CNO grid. These fits are displayed in Figure 7. We can see that in both cases we are able to reproduce the Balmer-line problem since in both cases the model grids we used are "inappropriate" for fitting the spectrum at hand. It should also be noted that the amount by which the atmospheric parameters are underestimated is larger in the first case ($\Delta T_{\rm eff} \approx 4000$ K, $\Delta \log g = 0.15$ dex, $\Delta \log {\rm He/H} = 0.10$ dex) than in the second. This suggests that the increase in CNO abundance has a smaller effect on the atmospheric parameter determinations than the inclusion of CNO altogether.

Having shown the necessity of computing models in NLTE and that the addition of CNO is compulsory in order to deal with

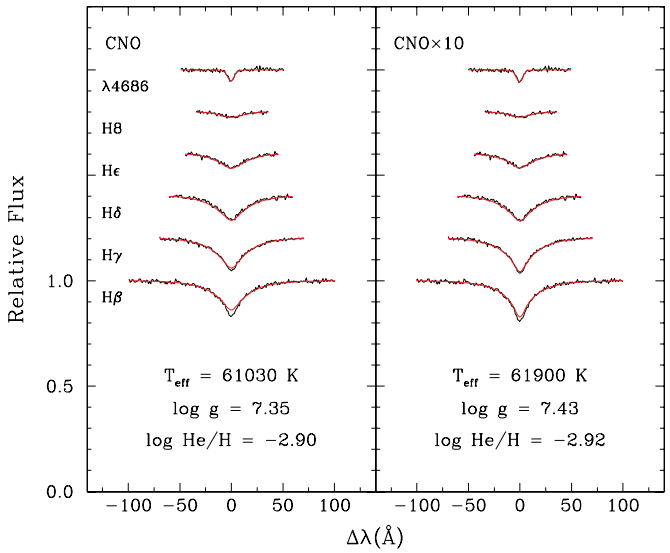

Figure 7. Fits of the Balmer lines from Hβ to Hϵ and He II λ4686 for models at $T_{\rm eff} = 65{,}000$ K, $\log g = 7.5$, and $\log {\rm He/H} = -3.0$. On the left, a synthetic spectrum computed from a model containing CNO was fit with a pure H/He grid. On the right, a synthetic spectrum computed from a model with a CNO abundance enhanced by a factor of 10 is fit with an H/He/CNO grid.

(A color version of this figure is available in the online journal.)

the Balmer-line problem, it is these models that we will use in order to analyze our sample of DAO white dwarfs. We should note that although the solution to the Balmer-line problem has been known since Werner (1996), several analyses of DAO white dwarfs have been performed without implementing it (Napiwotzki 1999; Hügelmeyer et al. 2007).

4. SPECTROSCOPIC ANALYSIS

4.1. Fitting Technique

Our fitting technique is identical to the one employed by Liebert et al. (2005) with the exception that we include the He II λ4686 line in addition to the Balmer lines from Hβ to H8. The first step is to normalize the flux from an individual line, in both observed and model spectra, to a continuum set to unity at a fixed distance from the line center. The comparison with model spectra, which are convolved with the appropriate Gaussian instrumental profile (3, 4, and 6 Å), is then carried out in terms of these line shapes only. The most sensitive aspect of this fitting technique is to define the continuum of the observed spectra. In this temperature range, we rely on theoretical spectra to reproduce the observed spectrum, including a wavelength shift, a zero point, as well as several order terms in λ (up to λ^6) using the nonlinear least-squares method of Levenberg–Marquardt (Press et al. 1986). The normal points are then fixed at the points defined by this smooth model fit. Note that the values of $T_{\rm eff}$, $\log g$, and log He/H at this stage are meaningless since too many fitting parameters are used, and the model just serves as a smooth fitting function to define the continuum of the observed spectrum. Once the lines are normalized to a continuum set to unity, we use our grid of model spectra to determine $T_{\rm eff}$, $\log g$, and log He/H in terms of these normalized profiles only. Our minimization technique again relies on the nonlinear least-squares method of Levenberg–Marquardt, which is based on a steepest descent method.

As we have shown in Section 2, several of the spectra contain emission lines that are due to the presence of a companion or a planetary nebula. These emission lines can affect both our determination of the continuum and the actual fit of the spectral lines. In order to avoid this problem, we have excluded the contaminated regions from our fits, both in terms of the normalization procedure and the fitting of the line profiles themselves. Furthermore, we have the four DAOZ white dwarfs whose spectra notably contain the C IV λ4658 line immediately blueward of He II λ4686. We have also omitted the spectral range where this line is found from our fits and extended the normalization region blueward of the C IV λ4658 line in order to properly determine the continuum for He II λ4686 in particular.

4.2. DAO White Dwarfs

Let us now examine the results obtained from combining the spectroscopic method described above with our new grid of NLTE model atmospheres that include CNO. We show in Figure 8 typical fits for several of our DAO white dwarfs. To better appreciate the difference between the models with and without CNO, we display in the top panels of Figure 8 fits with our NLTE H/He grid whereas the fits in the bottom panels are performed with our CNO grid. First and foremost, we note that the Balmer-line problem is no longer present when fitting with our CNO grid. Although this is a clear indication of the cooling effect of the CNO in the upper atmosphere, we would like to stress that this is by no means an indication of the abundance of CNO in the atmosphere.

Besides resolving the Balmer-line problem, we also obtain atmospheric parameters ($T_{\rm eff}$, $\log g$, and log He/H) that are significantly different in both cases, especially with respect to $T_{\rm eff}$ and $\log g$. In general, the fits with our CNO grid imply higher values for the surface temperature and gravity and slightly lower helium abundances. The fits without CNO tend to underestimate $T_{\rm eff}$ by ∼2000–5000 K and $\log g$ by ∼0.1–0.2 dex, which is in line with the differences we saw in Figure 7 when fitting a synthetic spectrum containing CNO with an H/He grid. As far as $T_{\rm eff}$ is concerned, the underestimate, when using the models without CNO, can be understood as the consequence of the fitting procedure attempting to reproduce the depth of the observed line profile and in this temperature regime that is accomplished by going to lower $T_{\rm eff}$. We will see below that the combined effect of higher $T_{\rm eff}$ and $\log g$ values shifts the position of DAO stars in the $T_{\rm eff}-\log g$ plane down toward the normal DA cooling sequence. This has important consequences for their possible evolutionary history.

Although the results displayed in Figure 8 are very encouraging, not all of the DAO stars in our sample produce the same results. Indeed, several DAO stars still show the Balmer-line problem even when fitting them with our CNO grid. In Figure 9, we present two such examples with 0127+581 and 2226−210. As we can see, even with the presence of CNO, the fits are not satisfactory although there is a definite improvement with respect to the grid without CNO, especially for 2226−210. In an attempt to fit these particular objects, we have computed a grid with the CNO abundances increased by a factor of 10 (CNO×10, see Figure 4). We can see that we obtain an excellent fit in both cases with this new grid of models. However, as we have stated before, the CNO we have included in our model atmospheres essentially acts as a proxy for all metals. It is perfectly reasonable to believe that simply increasing the abundance of CNO cannot mimic the effect other metals, like iron, for example, might have on the thermodynamic structure of the atmosphere, and consequently on the Balmer-line profiles. Furthermore, the abundances we are using for CNO (Asplund et al. 2005) are,

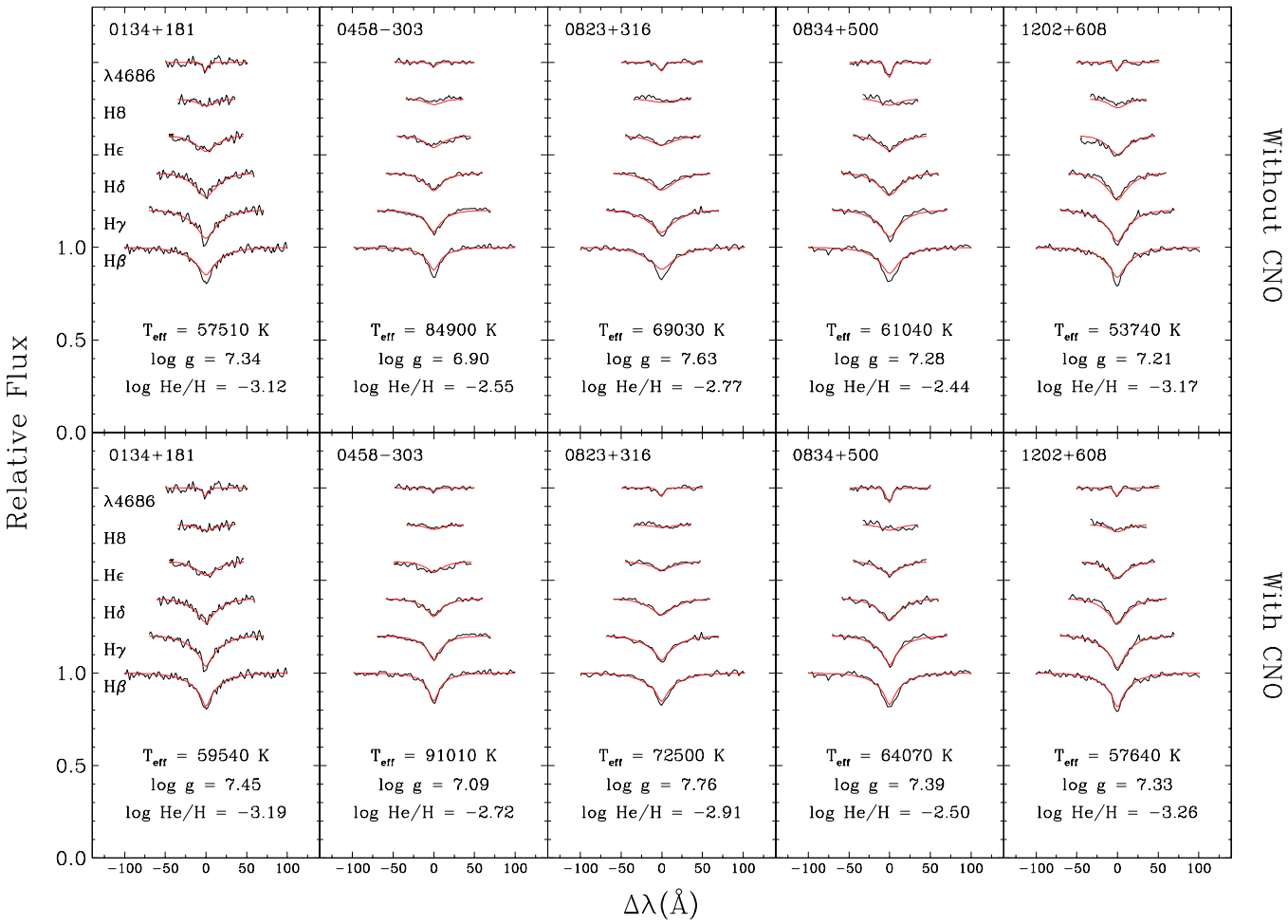

Figure 8. Typical fits of observed Balmer-line profiles and He II λ4686 for DAO white dwarfs. The fits in the top panels are performed with a grid of models assuming an H/He atmosphere. The fits in the bottom panels are performed using a grid of models containing H, He, and CNO. We clearly see how the inclusion of CNO improves the fits of Hβ and Hγ.

(A color version of this figure is available in the online journal.)

by all accounts, much too high as it is. Increasing them by an order of magnitude would then be even more unrealistic. For these reasons, the parameters we will adopt for our DAO white dwarfs are those obtained using our CNO grid only, even if this means that the Balmer-line problem will still be present, to varying degrees, in several of our fits.

On the other hand, a few DAOs either do not show the Balmer-line problem or we simply cannot tell whether the problem is present or not. 1013−050 and 1413+015 are fit perfectly with our H/He NLTE grid. Both of these stars are relatively cool and have higher log g values than all of the other DAO stars in our sample. The combination of age (i.e., lower $T_{\rm eff}$) and higher surface gravity has likely allowed any surplus of metals to diffuse out of the atmosphere. 2011+398 is similarly cool and massive, however emission in the line cores from its M dwarf companion prevents us from determining whether the Balmer-line problem is actually present. However, parameters obtained with our H/He NLTE and CNO grids are virtually identical for this star. This is not at all surprising since in both cases we are only fitting the line wings where the presence, or lack thereof, of CNO in the atmosphere is essentially irrelevant since the line wings form deeper in the atmosphere where the effect of CNO is negligible. For these reasons, we adopt the parameters obtained from our H/He grid for 2011+398 as well. The case of 0950+139 is similar in that there is also emission in the line core but due to the surrounding planetary nebula this time. We will see below that the parameters for this star place it squarely in the realm of DAO white dwarfs that exhibit the Balmer-line problem. Consequently, we adopt the parameters from our CNO grid for this object.

We now wish to address the particular case of PG 1210+533. Bergeron et al. (1994) had encountered difficulties in fitting the He II λ4686 line profile for this star. Indeed, neither homogeneous nor stratified models allowed for satisfactory fits to the observed He II λ4686 line profile. In both cases, the theoretical line profiles were predicted to be too shallow (see Bergeron et al. 1994, Figure 6). As per their own suggestion that PG 1210+533 required further monitoring, a new spectrum of this star was obtained in 1994 January. We display in Figure 10 fits to the He II λ4686 line from the two separate observations using the LTE models employed by Bergeron et al. (1994) and our new NLTE models containing CNO. We see that for the 1992 April observation, neither set of models can properly reproduce the observed line profile although the newer models do a slightly better job. In contrast, both model grids have no difficulty in fitting the He II λ4686 line profile of the 1994 January observation. As such, we conclude that the issue encountered by Bergeron et al. (1994) can be attributed to the spectroscopic variability of

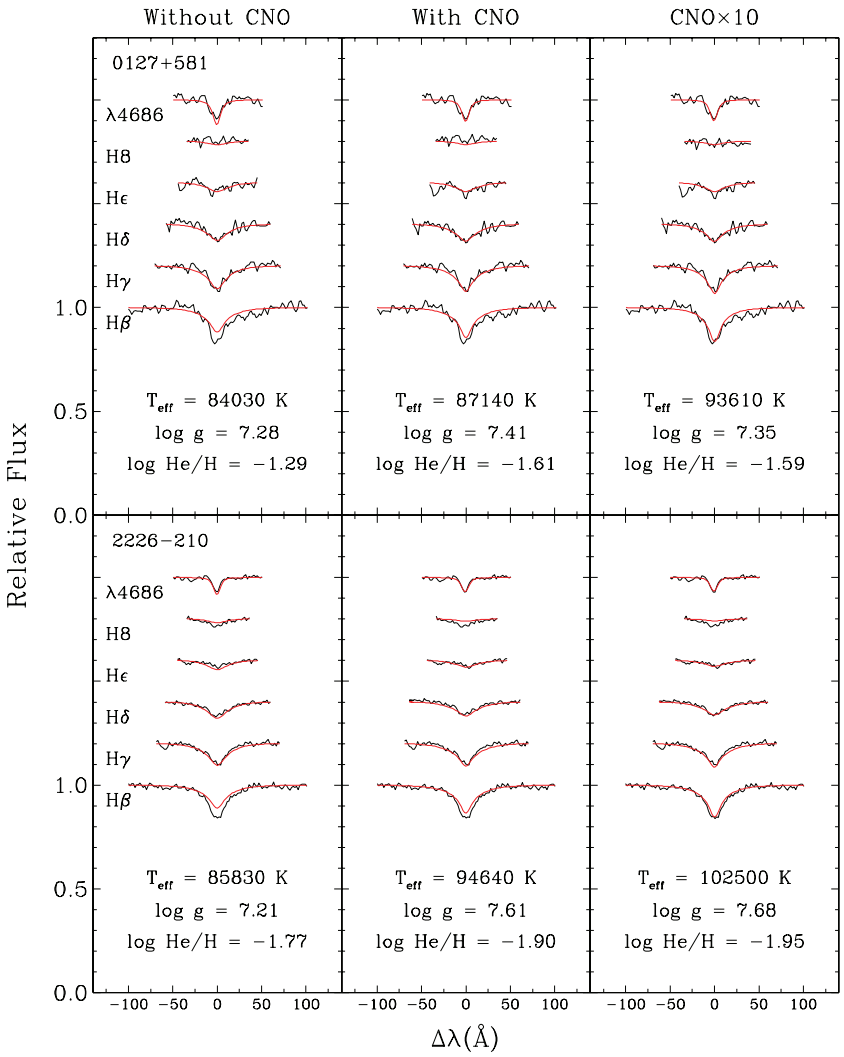

Figure 9. Fits to the observed Balmer-line profiles and He II λ4686 for 2 DAO white dwarfs, 0127+581 (top) and 2226−210 (bottom). Fits from left to right are performed with increasing abundances of CNO from none (left), to solar (middle), and finally 10 times solar (right).

(A color version of this figure is available in the online journal.)

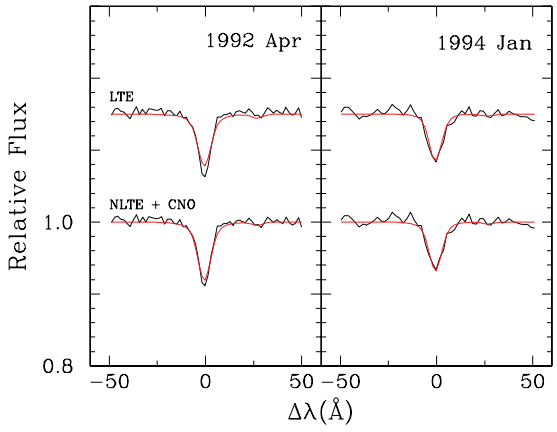

Figure 10. Fits to the He II λ4686 line profile of PG 1210+533 for spectra taken in 1992 April (left) and 1994 January (right) using models computed in LTE (top) and models computed in NLTE that also include CNO (bottom).

(A color version of this figure is available in the online journal.)

PG 1210+533, which will be discussed in Section 6, more so than any inadequacy of the models they were using.

Finally, the only DAO white dwarf that was successfully modeled with a stratified atmosphere by Bergeron et al. (1994) was PG 1305−017. Our new model grid is thus inappropriate for analyzing this particular object and as such, we adopt the atmospheric parameters they obtained for this star.

4.3. Hot DA White Dwarfs

In addition to the DAO white dwarfs, Bergeron et al. (1994) also analyzed 29 hot DA stars. In particular, they studied the effects that spectroscopically invisible traces of helium would have on the Balmer-line profiles and consequently on the determination of the atmospheric parameters for those stars. Of course, as we have seen, when models are computed in NLTE, the addition of helium has no discernible effect on the Balmer lines of hot DA white dwarfs. As such, there is no evidence to suggest that these stars contain helium in their atmospheres and one could thus conclude that DAO stars form a class of objects that is quite distinct from the DA white dwarfs found in the same temperature regime. Indeed, of the 29 hot DA stars analyzed by Bergeron et al. (1994), the Balmer-line problem did not manifest itself in any of them. As such, Bergeron et al. (1994) concluded that the Balmer-line problem must be unique to DAO stars. On

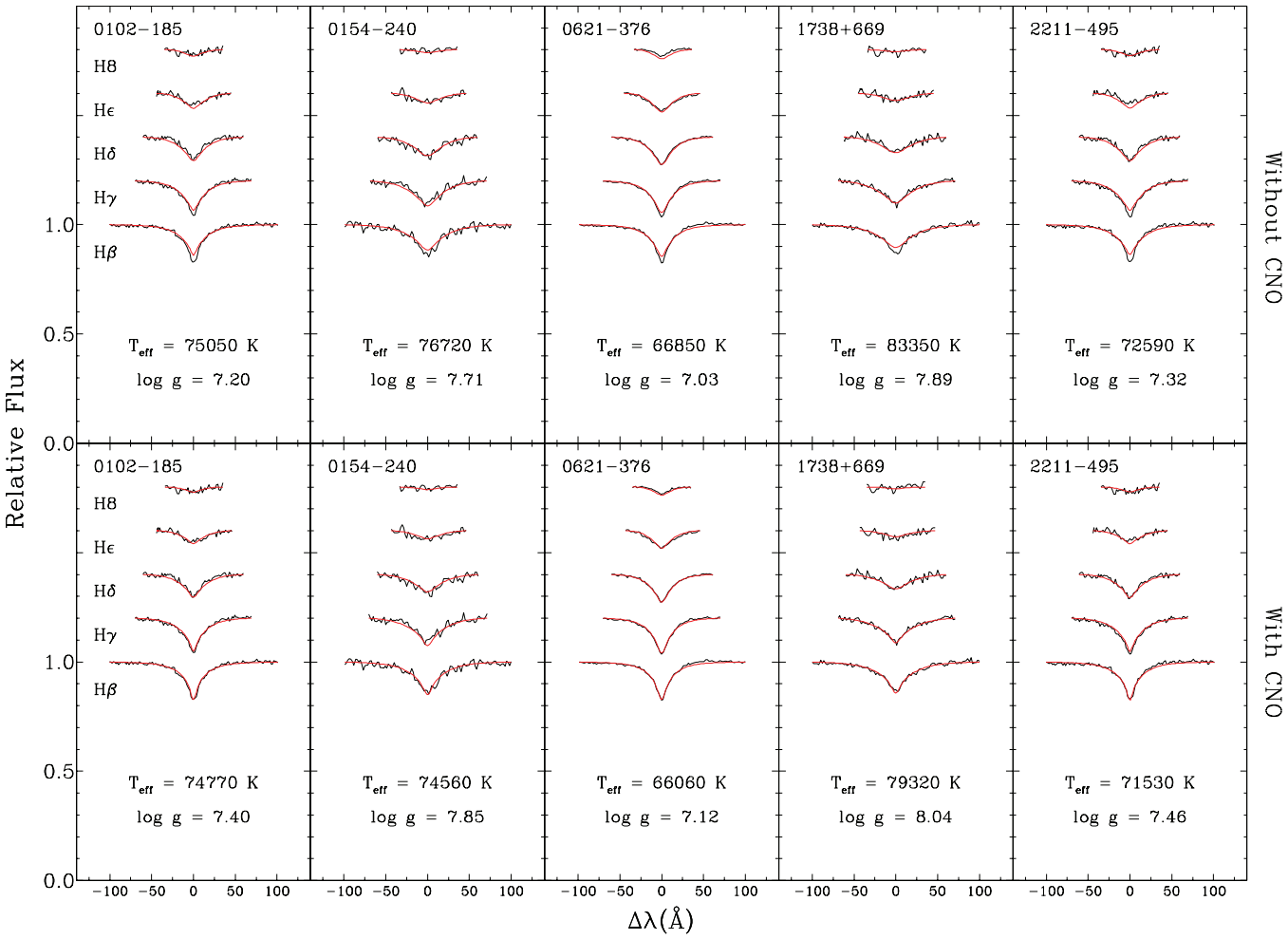

Figure 11. Same as Figure 8 but for DA white dwarfs showing the Balmer-line problem.
(A color version of this figure is available in the online journal.)

the other hand, our ongoing survey (Gianninas et al. 2009) has provided us with a sample of 152 white dwarfs with $T_{\rm eff} >$ 40,000 K. With a sample over five times larger than that of Bergeron et al. (1994), we have discovered that 18 of these hot DA white dwarfs are also afflicted with the Balmer-line problem (hereafter DA+BP), just like their DAO counterparts.

This is not the first time that this problem has been reported in stars other than DAO stars. There was a note added at the end of Bergeron et al. (1994) regarding the detection of the Balmer-line problem in 0948+534. Vennes (1999) also reported observing the Balmer-line problem in 0621−376 (EUVE J0623−376) and 2211−495 (EUVE J2214−493), both of which are in our sample. However, there was never any follow-up to these detections in subsequent works. A search of the literature also turned up a case where the Balmer-line problem can be seen but is not reported or discussed by the authors: 0556−375 (EUVE J0558−375; Vennes et al. 1997, see their Figure 2). We should also mention that 2218+706 was shown to exhibit the Balmer-line problem by Barstow et al. (2001a). However, 2218+706 was later deemed to be a DAO star (see Section 2.1) and so the Balmer-line problem in regular DA white dwarfs remained a non-issue.

In similar fashion to the previous section, we show in Figure 11 typical fits to five of the hot DA stars that we have found to exhibit the Balmer-line problem. The top panels show fits performed using a grid of pure H atmospheres computed in NLTE and we can clearly see the inability of these models to fit the core of Hβ. In the bottom panels, we show an identical analysis but here we use a grid analogous to our CNO grid for the DAO stars but without the presence of helium. We see once again that the inclusion of CNO in the models allows us to overcome the Balmer-line problem and adequately fit the line profiles of these stars with the exception of two that are discussed below. As far as the new atmospheric parameters obtained, we note that log g is systematically higher for all the stars in Figure 11 and indeed for all 18 hot DA stars exhibiting the Balmer-line problem, as was the case for the DAO stars. However, unlike the DAO stars, which yielded systematically higher temperatures when fit with the CNO grid, most of the hot DAs curiously yield lower temperatures. This dichotomy in the shifts of $T_{\rm eff}$ values when fitting with and without CNO in the models for DA and DAO white dwarfs can be ascribed to the presence of helium. We took synthetic spectra computed with CNO and fit them with our grid that does not contain any metals in order to examine the systematic differences in the derived atmospheric parameters while assuming different helium abundances. The results of this exercise are presented in Figure 12. The dots represent the correct values for the CNO models while the vectors point to the values obtained from the fits for He/H = 0, 10^{-4}, and 10^{-2}. As observed in the actual fits of our observed spectra, all the solutions underestimate the true surface gravity when fitting without CNO in the models. What is more interesting is the

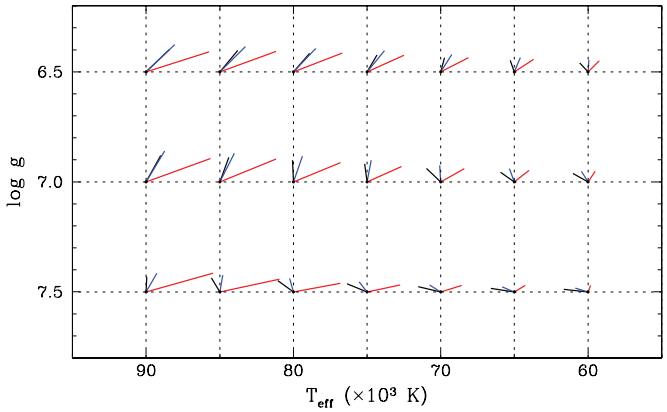

Figure 12. Results from the fits of our CNO grid (dots) using a grid that does not contain any metals. The vectors point to the values obtained from the fits with He/H = 0 (black), 10^{-4} (blue), and 10^{-2} (red). The shifts in temperature have been reduced by a factor of two for clarity.

(A color version of this figure is available in the online journal.)

behavior as we change the helium abundance. The difference vectors "rotate" in the $T_{\rm eff}$–log g plane from left to right as the helium abundance is increased. In other words, stars analyzed with CNO models will yield lower temperatures in cases where there is no helium (DA stars) but higher temperatures when sufficient helium is present (DAO stars), which is exactly what we observe in the fits of our spectroscopic sample.

As we did in Figure 9, we show in Figure 13 fits using three different model grids (H/He only, CNO, and CNO ×10) for the only two hot DA stars that still exhibit a case of the Balmer-line problem despite the addition of CNO: 0237+241 and 0311+480. As in the case of the DAO stars, the increasing metal abundance produces successively better fits to the observed line profiles. Curiously, these are the only two DA+BPs where $T_{\rm eff}$ actually increases with the addition of CNO. As with the DAO stars, although the fits with the CNO×10 grid are qualitatively better, we adopt the atmospheric parameters from the CNO fits for these two stars for the same reasons outlined earlier. The reason why these two stars in particular would show a more acute case of the Balmer-line problem is not immediately obvious but there is a clue in each case as to the cause of this discrepancy. A closer inspection of the optical spectrum of 0247+241 reveals what seem to be metallic absorption lines near Hϵ. With an abundance of metals large enough to produce absorption lines

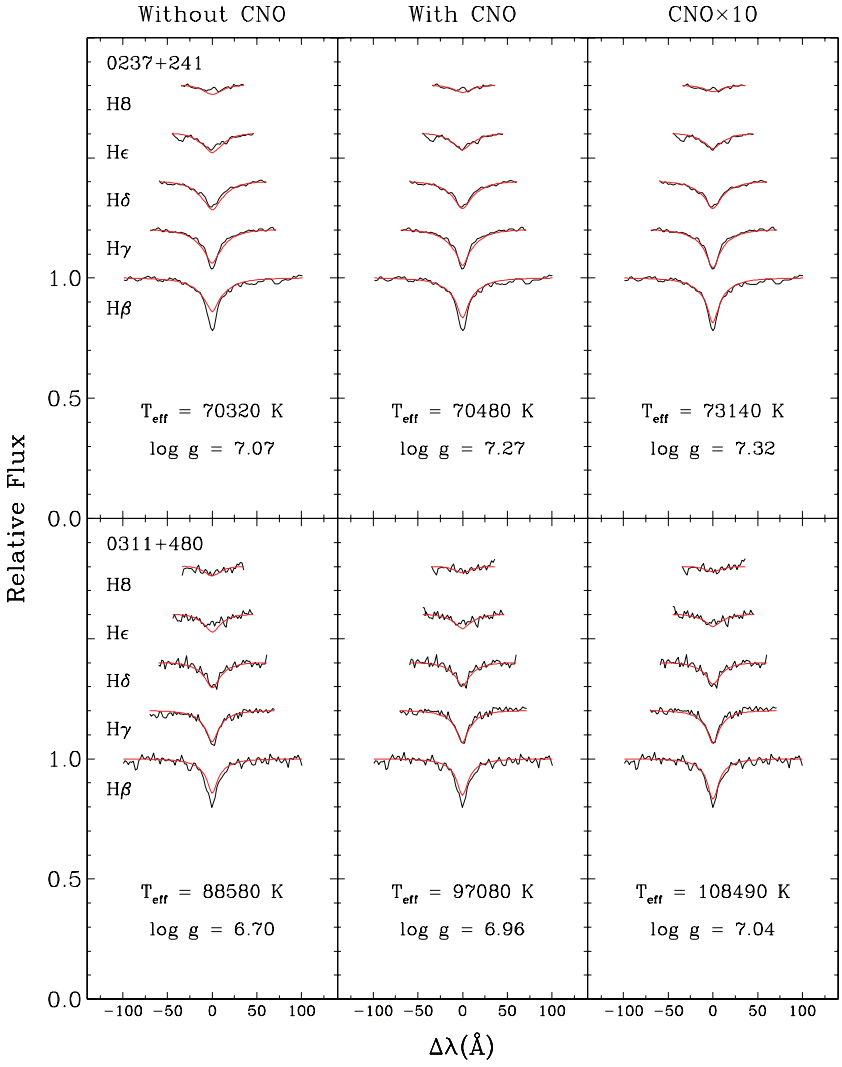

Figure 13. Fits to the observed Balmer-line profiles for two DA white dwarfs, 0237+241 (top) and 0311+480 (bottom). Fits from left to right are performed with increasing abundances of CNO from none (left), to solar (middle), and finally 10 times solar (right).

(A color version of this figure is available in the online journal.)

Table 2
Atmospheric Parameters of DAO White Dwarfs

WD	Name	$T_{\rm eff}$ (K)	log g	log He/H	$M/M_{\odot}$	M_V	Ref.	Notes
0127+581	Sh 2–188	87140	7.41	−1.61	0.58	7.20	1	CSPN
0134+181	PG 0134+181	59540	7.45	−3.18	0.51	7.83	2	
0231+050	PG 0231+051	89470	7.52	−1.95	0.62	7.42	3	
0322+452	HDW 3	91200	7.32	−1.29	0.57	6.95	1	CSPN
0439+466	LS V +46 21	86980	7.23	−2.10	0.54	6.83	1	CSPN
0458−303	MCT 0458−3020	91010	7.09	−2.72	0.53	6.46	4	
0500−156	A66 7	82710	7.47	−1.36	0.59	7.43	5	CSPN
0505+012	HS 0505+0112	60340	7.67	−1.09	0.58	8.25	3	DAOZ
0615+556	PuWe 1	93150	7.57	−1.65	0.64	7.42	1	CSPN
0823+316	Ton 320	72500	7.76	−2.91	0.64	8.16	6	CSPN
0834+500	PG 0834+501	64070	7.39	−2.50	0.51	7.61	7	
0846+249	Ton 353	70180	7.48	−3.37	0.55	7.67	6	
0950+139	PG 0950+139	93230	7.36	−1.60	0.59	7.00	8	CSPN, emission
1013−050	RE J1016−053	57250	8.03	−3.54	0.72	8.93	9	DA + dM, no CNO
1136+667	HS 1136+6646	83090	7.31	−2.36	0.55	7.06	3	DA + dK
1201−049	PG 1201−049	57260	7.61	−3.46	0.55	8.19	4	DAOZ
1202+608	Feige 55	57640	7.33	−3.26	0.47	7.65	10	Double degenerate
1210+533	PG 1210+533	46320	7.88	−2.20	0.63	8.98	7	Spectroscopic variable
1214+267	LB 2	67850	7.72	−2.79	0.62	8.18	2	
1253+378	HZ 34	87670	7.02	−1.81	0.50	6.38	7	
1305−017	PG 1305−017	44400	7.76	...	0.57	8.80	7	Stratified
1413+015	PG 1413+015	47770	7.72	−2.56	0.56	8.64	11	DA+dM, no CNO
1822+008	Sh 2–68	84460	7.24	−0.86	0.53	6.93	1	CSPN, DAOZ
1957+225	NGC 6853	86670	7.36	−1.29	0.57	7.13	1	CSPN
1958−501	BPS CS 30302-17	56870	7.97	−3.55	0.69	8.85	4	
2011+398	RE J2013+400	49650	7.94	−2.79	0.66	8.97	12	DA+dM, emission, no CNO
2115+118	HS 2115+1148	62230	7.76	−2.97	0.62	8.36	13	DAOZ
2226−210	NGC 7293	94640	7.61	−1.90	0.65	7.49	1	CSPN
2342+806	GD 561	74160	7.16	−2.65	0.48	6.94	14	CSPN, binary

References. (1) Napiwotzki 1995; (2) Bergeron et al. 1994; (3) Heber et al. 1996; (4) this work; (5) Greenstein 1984; (6) Kidder et al. 1991; (7) Green et al. 1986; (8) Liebert et al. 1989; (9) Barstow et al. 1993; (10) Lamontagne et al. 1993; (11) Fulbright et al. 1993; (12) Barstow et al. 1995; (13) Dreizler et al. 1995a; (14) Bergeron et al. 1992.

Table 3
Atmospheric Parameters of Hot DA White Dwarfs with the Balmer-Line Problem

WD	Name	$T_{\rm eff}$ (K)	log g	$M/M_{\odot}$	M_V
0102−185	PHL 975	74770	7.40	0.54	7.56
0113−245	KUV 01138−2431	58880	7.56	0.54	8.19
0154−240	PHL 1248	74560	7.85	0.68	8.46
0237+241	PG 0237+242	70480	7.27	0.50	7.38
0311+480	KPD 0311+4801	97080	6.96	0.53	6.23
0455−282	RE J0457−280	63540	7.58	0.56	8.14
0615+655	HS 0615+6535	77780	7.93	0.72	8.58
0621−376	RE J0623−374	66060	7.12	0.45	7.19
0915+201	LB 3016	72710	7.49	0.56	7.79
0948+534	PG 0948+534	139500	7.56	0.75	7.04
1328−152	EC 13288−1515	57980	7.89	0.66	8.83
1401+005	PG 1401+006	63530	7.88	0.68	8.70
1526+013	PG 1526+013	50000	7.89	0.64	8.99
1532+033	PG 1532+034	66610	7.67	0.60	8.25
1738+669	RE J1738+665	79320	8.04	0.77	8.76
2146−433	MCT 2146−4320	78090	7.30	0.53	7.31
2211−495	RE J2214−491	71530	7.46	0.55	7.74
2218+706	DeHt 5	76750	7.38	0.54	7.48

in the optical, it is then not surprising that 0247+241 should display a more severe form of the Balmer-line problem. On the other hand, 0311+480 is the DA+BP star with the lowest log g measurement in which the Balmer-line problem manifests itself. It is therefore not unlikely that the lower gravity allows for a larger quantity of metals to be supported in the star's atmosphere by radiation pressure, thus causing a more severe case of the Balmer-line problem as well.

4.4. Atmospheric Parameters

The atmospheric parameters we have adopted for the DAO stars in our analysis are summarized in Table 2 where we list the values of $T_{\rm eff}$, log g, and log He/H determined from our spectroscopic fits using our CNO grid as well as the masses derived from the evolutionary models of Wood (1995) with thick hydrogen layers, and absolute visual magnitudes determined using the photometric calibrations from Holberg & Bergeron (2006). We list, as a reference, the sources where each of these white dwarfs was first identified as belonging to the DAO spectral type. Additionally, we also indicate which objects are known CSPN, which parameters were determined using only our H/He NLTE grid, which stars contain emission lines in their optical spectrum, which stars are in binary systems, and finally we identify those stars that are of the DAOZ spectral type. Furthermore, since we have opted to use the atmospheric parameters from Bergeron et al. (1994) for PG 1305−017, this means we do not have a measurement of the helium abundance for this star. This is because the fit by Bergeron et al. (1994) using their stratified models used, instead, a quantity related to the thickness of the hydrogen layer as a free parameter. In Table 3, we list the atmospheric parameters, masses, and absolute visual magnitudes obtained for the DA+BP stars. All of these results are summarized in Figure 14 where we plot the location in the

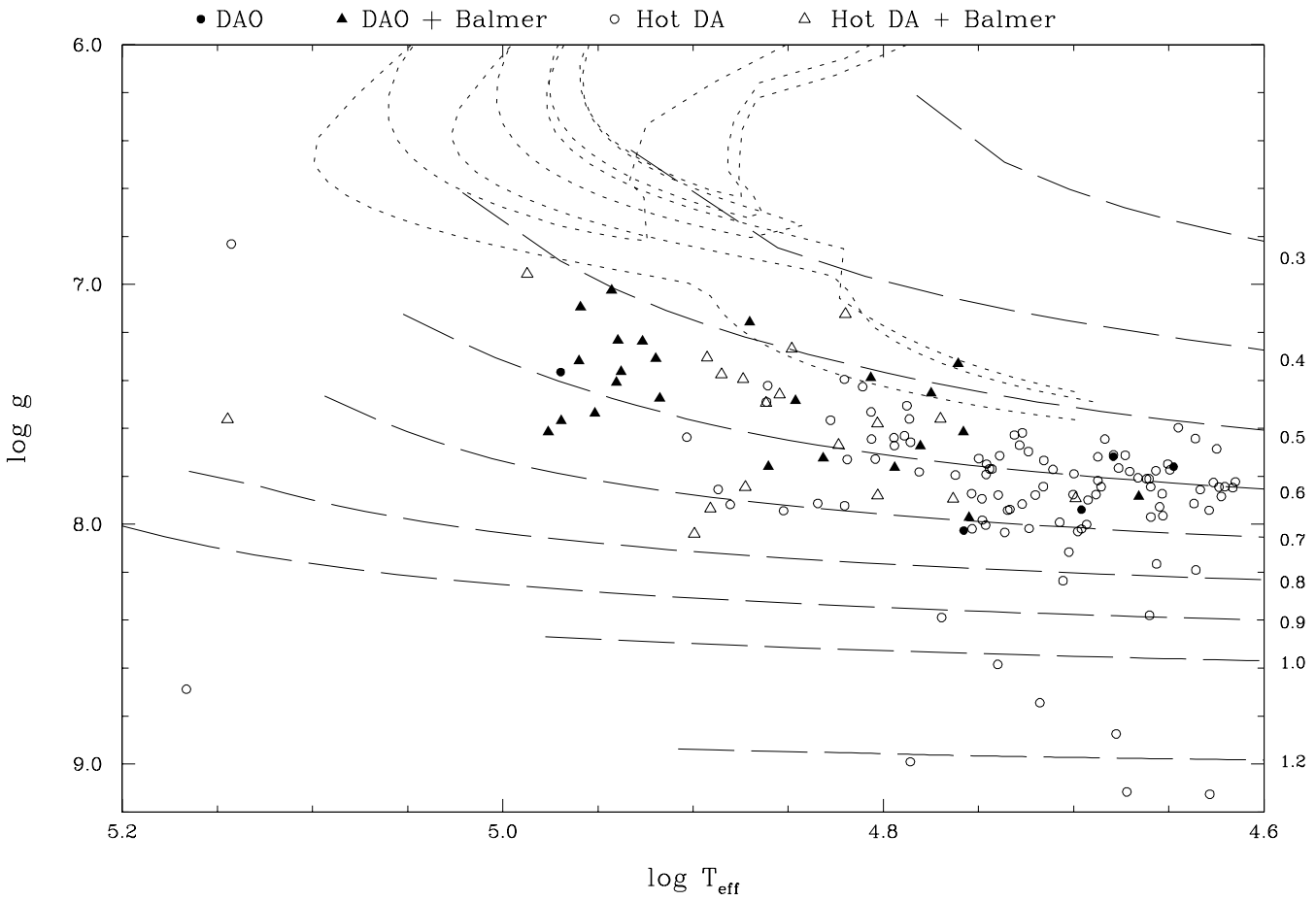

Figure 14. Section of the log g vs. log $T_{\rm eff}$ diagram showing the hot end of the DA white dwarf cooling sequence. Open symbols correspond to DA white dwarfs whereas filled symbols represent DAO white dwarfs. Triangles correspond to stars exhibiting the Balmer-line problem. The dashed lines represent white dwarf cooling tracks with thick hydrogen layers from Wood (1995) and are labeled with their mass (in solar mass units) to the right of the figure. The dotted lines are three evolutionary tracks from Dorman et al. (1993). From top to bottom, a 0.471 $M_{\odot}$ and 0.475 $M_{\odot}$ post-EHB tracks and a 0.495 $M_{\odot}$ post-EAGB evolutionary track.

log $T_{\rm eff}$−log g plane of the 29 DAO white dwarfs, 18 DA+BP stars, and the remaining 104 hot DA white dwarfs from our sample. The filled and open symbols represent the DAO and DA white dwarfs, respectively, whereas the triangles denote stars where the Balmer-line problem has been detected. The dashed lines represent cooling sequences from Wood (1995) for C/O core white dwarfs with thick hydrogen layers and they are labeled by their values of stellar mass. We note that these cooling sequences use post-AGB evolutionary sequences as a starting point (M. A. Wood 2010, private communication). We also plot, as dotted lines, two post-extreme horizontal branch (post-EHB) evolutionary sequences at 0.471 and 0.475 $M_{\odot}$ as well as a post-early asymptotic giant branch (post-EAGB) sequence at 0.495 $M_{\odot}$. These represent stars that left the AGB before the thermally pulsing stage (Dorman et al. 1993). The above three sequences are taken from Dorman et al. (1993) and all of them assume [Fe/H] = 0.

One of the first things we note is that most, but not all, of the hottest white dwarfs are DAO stars. More importantly, the sequence of DAO white dwarfs seems to seamlessly join the normal DA cooling sequence. This would suggest that the majority of these stars share a common evolutionary history. This is a very different result from that obtained by Bergeron et al. (1994) who had suggested that DAO white dwarfs might, instead, be the product of stars having evolved directly from the EHB (post-EHB evolution) to the white dwarf phase unlike most white dwarfs, which are descendants of stars having evolved off the AGB (post-AGB evolution). This new result is a direct consequence of the new parameters we have obtained, which make DAO white dwarfs hotter, and more importantly, more massive than previously measured. As mentioned above, our grid of model spectra makes use of the improved Stark profiles developed by Tremblay & Bergeron (2009). A comparison of our grids with analogous grids computed with the older tables of Lemke (1997) reveals that temperatures increase, on average by about 3%, and the log g values by ∼0.05 dex (see also Figure 8 of Tremblay & Bergeron 2009). However, these shifts in the atmospheric parameters are smaller than those brought on by the inclusion of CNO in the models. More importantly, the use of the new tables from Tremblay & Bergeron (2009) alone would not have allowed us to overcome the Balmer-line problem. Clearly, the addition of metals is the dominant factor to consider in comparing our results and conclusions with those of Bergeron et al. (1994).

With that being said, we must also note that there are a few stars in Figure 14 with somewhat lower masses. First of all, the DAO white dwarf with the lowest mass (0.47 $M_{\odot}$), Feige 55, is a known double-degenerate system (Holberg et al. 1995). As such, it is highly likely that it has lost mass through interactions with its companion, which Holberg et al. (1995) conclude is likely a less luminous white dwarf. Another noteworthy star is GD 561 (2342+806) at log $T_{\rm eff}$ ∼ 4.87 and just above the 0.5 $M_{\odot}$

cooling track. Interestingly, GD 561 has a known planetary nebula (Sh 2–174; Napiwotzki & Schönberner 1993). Based on their results, Bergeron et al. (1994) had suggested that GD 561 could represent a case where post-EHB evolution produced a planetary nebula by way of H-flashes late in the star's evolution. However, Napiwotzki (1995) later discovered that GD 561 actually has a cool companion separated by $\approx 4''$. In addition, Napiwotzki (1995) reported the detection of a slight excess in the *K* band that also supports a binary scenario for this object. The exact nature of the companion has never been determined, to our knowledge. Later, Saffer et al. (1998) observed GD 561 in an effort to determine if it was a radial velocity variable but no variations were detected. Good et al. (2005a) did not detect any significant radial velocity variations either. Regardless, the binary nature of GD 561 likely explains why this star has a lower mass and the presence of the planetary nebula seems to point toward the canonical post-AGB evolution for white dwarfs. As such, the post-EHB scenario suggested by Bergeron et al. (1994) need no longer be invoked. The other lower mass object is 0621−376 (0.45 $M_{\odot}$), a DA+BP white dwarf. This star seems to be consistent with post-EHB evolution as it falls almost on top of the two post-EHB sequences plotted. However, this solitary object does not change our original conclusion that most of the stars in our sample, DA and DAO, are descendants from post-AGB evolution. Finally, it should also be pointed out that several stars near the 0.50 $M_{\odot}$ cooling sequence could also be compatible with the post-EAGB evolutionary scenario.

With respect to the Balmer-line problem, we see in Figure 14 that it is found mostly in the hotter stars although not in all of them, and there are also a few cooler stars that are also afflicted. More importantly, *all* the hot DAO stars exhibit the Balmer-line problem with the exception of the previously discussed case of PG 0950+139. Of the other four DAO white dwarfs that do not show the Balmer-line problem, the coolest one is PG 1305−017, which represents the only case of a stratified atmosphere. The other three cool white dwarfs that do not display the Balmer-line problem are 1013−050, 1413+015, and 2011+398. These three stars are members of DA+dM binary systems (probably pre-cataclysmic variables (CVs)). It is likely that in the case of these stars, the helium observed in the spectrum of the white dwarf primary results from interactions with their M dwarf companion. The helium could have been accreted from the companion star or the system may have undergone a common envelope phase during which much of the white dwarf's hydrogen was stripped away. In the latter case, even a moderate mass-loss rate could bring sufficient helium to the surface of the star. As we will discuss later, there is likely a link between the fact that these three stars do not show the Balmer-line problem and that the source of their helium is the result of their membership in DA+dM binary systems. The coolest DAO star showing the Balmer-line problem is PG 1210+533, unique among DAO white dwarfs in that it displays spectroscopic variability. It is interesting to note that PG 1210+533 and PG 1305−017, possibly the two most unique DAO white dwarfs, are the only ones where the He II λ1640 line has been detected in their UV spectra.

We now turn our attention to the DA white dwarfs in Figure 14. We first remark that the DA+BP stars are all hotter than ∼55,000 K (log $T_{\rm eff} \sim 4.75$). The lone exception to this rule is 1526+013 (log $T_{\rm eff} \sim 4.7$). However, our spectrum for 1526+013 has a somewhat lower S/N and this makes the detection of the Balmer-line problem more difficult. It is thus quite possible that 1526+013 does not suffer from the Balmer-line problem at all. More importantly, the DA+BP white dwarfs do not seem to dominate over their normal DA counterparts. Specifically, in the range $4.8 < \log T_{\rm eff} < 4.9$, there seem to be just as many normal DA stars as DA+BP stars. This would seem to imply a transition region where the phenomenon responsible for the Balmer-line problem slowly ceases to operate. As we have already noted, most of the hottest stars are DAO white dwarfs but there also four very hot DA white dwarfs among them. Of these four stars, two are normal DAs while the other two are DA+BP stars. The two DA white dwarfs are 0556+106 and 2246+066. 0556+106 is actually a CSPN (Liebert et al. 1994) while 2246+066 was discovered during the course of the Hamburg Quasar Survey (Homeier et al. 1998). As for the two very hot DA+BPs, 0311+480 represents one of the two extreme cases of the Balmer-line problem in DA stars as shown in Figure 11. On the other hand, despite being the hottest DA+BP star (log $T_{\rm eff} \sim 5.15$), and consequently having rather shallow Balmer lines to begin with, we do detect the Balmer-line problem in 0948+534 as well.

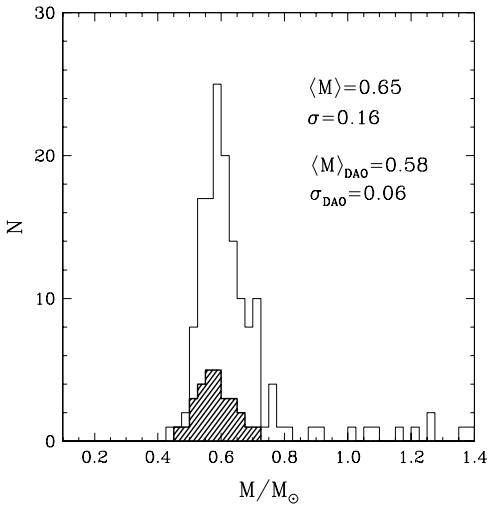

Figure 15. Mass distribution for our entire sample of hot white dwarfs (solid line histogram) and of the DAO white dwarfs (hatched histogram).

In Figure 15, we display the mass distribution of our entire sample of hot white dwarfs as compared to that of the 29 DAO stars. We see that the mass distribution of the whole sample is strongly peaked around ∼0.6 $M_{\odot}$ with a mean mass of 0.65 $M_{\odot}$ and a dispersion of 0.16 $M_{\odot}$. The dispersion would probably be lower were it not for the presence of a number of higher mass white dwarfs in the sample. The hatched histogram shows the mass distribution for the DAO stars only. The latter is strongly peaked around ∼0.55−0.60 $M_{\odot}$ with a mean of 0.58 $M_{\odot}$ and a dispersion of 0.06 $M_{\odot}$. Although the mean mass is lower than that of the whole sample it is not uncomfortably lower. Indeed, if we take into account the dispersions of each distribution, both mass distributions are consistent with a single population of white dwarfs. This is yet another strong indication that most DAO white dwarfs stem from the same evolutionary channel as their DA brethren.

5. FUSE OBSERVATIONS

In this section, we turn our attention to the FUV spectra of these hot white dwarfs. We have seen that the inclusion of CNO in our models greatly improves the fits for both DA and DAO stars that suffer from the Balmer-line problem, and we now wish to understand its underlying causes. To this end, we will make

Table 4
List of *FUSE* Observations

WD	Name	Exposures	Exposure Time (s)	Aperture
0001+433	RE J0003+433	18	26827	LWRS
0004+330	GD 2	79	83276	LWRS/MDRS
0027−636	RE J0029-632	5	14619	LWRS
0131−163	PHL 1043	4	8619	LWRS
0229−481	LB 1628	4	10704	LWRS
0343−007	KUV 03439−0048	2	3869	LWRS
0346−011	GD 50	21	43407	LWRS
0421+740	RE J0427+741	16	61145	LWRS
0455−282	RE J0457−280	31	47464	MDRS
0501+527	G191-B2B	149	68575	LWRS/MDRS
0505+012	HS 0505+0112	4	7111	LWRS
0615+655	HS 0615+6535	17	30146	LWRS
0621−376	RE J0623−374	40	18147	LWRS
0718−316	RE J0720-318	6	17659	LWRS
0802+413	KUV 08026+4118	4	9163	LWRS
0823+316	Ton 320	9	8427	LWRS
0834+500	PG 0834+501	4	9730	LWRS
0948+534	PG 0948+534	5	10855	LWRS
0950+139	PG 0950+139	11	21418	LWRS
1029+537	RE J1032+532	5	7408	LWRS
1040+492	RE J1043+490	63	57466	LWRS
1057+719	PG 1057+719	13	34203	LWRS
1136+667	HS 1136+6646	4	14098	LWRS
1202+608	Feige 55	36	49096	LWRS/MDRS
1210+533	PG 1210+533	3	4597	LWRS
1214+267	LB 2	6	9209	LWRS
1234+481	PG 1234+482	20	31542	LWRS
1253+378	HZ 34	7	7474	LWRS
1302+597	GD 323	7	17448	LWRS
1314+293	HZ 43	120	66227	LWRS/MDRS
1342+443	PG 1342+444	4	10679	LWRS
1444+636	RE J1446+632	8	10720	LWRS
1528+487	RE J1529+483	50	46737	LWRS/MDRS
1611−084	RE J1614−083	6	9643	LWRS
1631+781	RE J1629+780	32	57347	LWRS/MDRS
1711+668	RE J1711+664	16	35002	LWRS
1725+586	LB 335	7	18154	LWRS
1738+669	RE J1738+665	14	33648	LWRS
1740−706	RE J1746−703	27	56187	LWRS
1800+685	KUV 18004+6836	23	63824	LWRS
1819+580	RE J1820+580	8	5411	LWRS
1950−432	MCT 1950−4314	7	14779	LWRS
2004−605	RE J2009−605	11	9718	LWRS
2011+398	RE J2013+400	95	73695	LWRS/MDRS
2046+396	KPD 2046+3940	4	8812	LWRS
2116+736	KUV 21168+7338	13	55373	LWRS
2124−224	BPS CS 29506-51	25	18938	MDRS
2146−433	MCT 2146−4320	10	13690	LWRS
2211−495	RE J2214−491	198	91639	LWRS/MDRS
2218+706	DeHt 5	3	6056	LWRS
2247+583	Lanning 23	18	62033	LWRS
2309+105	BPM 97895	91	45617	LWRS/MDRS
2321−549	RE J2324-544	6	14471	LWRS
2353+026	PB 5617	4	5604	LWRS

use of FUV spectra from the FUSE archive.[6] The spacecraft and instrumentation are described in Moos et al. (2000, 2002). We retrieved spectra from the archive for as many of the DAO and hot DA stars in our sample that we could find. In total, we were able to obtain spectra for 10 of our DAO white dwarfs, 8 of the DA+BP stars, and 53 for the rest of our hot DA stars.

[6] http://archive.stsci.edu/fuse/

Table 5
Selected Wavelength Intervals and Central Wavelengths in *FUSE* Data

Ions	Wavelength Interval (Å)	Central Wavelengths (Å)
C IV	1106.5–1109.5	1107.59
...	...	1107.93
...	...	1107.98
N IV	921.5–924.5	921.99
...	...	922.52
...	...	923.05
...	...	923.22
...	...	923.68
...	...	924.28
O VI	1030.5–1033.5	1031.91
P V	1126.5–1129.5	1128.01
Si IV	...	1128.34
P V	1116.5–1119.5	1117.98
S VI	931.5–934.5	933.38
Fe VI/Fe VII	1164.5–1167.5	1165.10
...	...	1165.70
...	...	1166.18

The list of FUSE observations is presented in Table 4 where we indicate the number of exposures, total exposure time, and the aperture(s) used. The data provide a wavelength coverage from ∼905 to 1185 Å, and the majority of the observations were obtained using the low-resolution LWRS aperture that provides a resolution of $R \sim 20{,}000$. The spectra were processed using the latest version of the calibration pipeline, CalFUSE 3.2.3 (Dixon et al. 2007). The processed spectra were then co-aligned from individual exposures by cross-correlating the spectra in pixel space over small regions that include narrow absorption lines. Finally, the spectra were combined by taking an exposure-weighted average of all observations.

FUSE spectra have already been exploited in an effort to study DAO white dwarfs in a series of papers by Good et al. (2004, 2005a, 2005b). In particular, Good et al. (2005a) fit several of the observed metallic lines in the *FUSE* spectra with a grid of models whose metallicities were scaled to the measured abundances in G191-B2B. DA stars have also been the target of numerous studies aimed at determining the abundances of metals present in their atmospheres. Our analysis of the available FUV data will be a qualitative one as we are not interested in determining metal abundances for each individual star. Rather, our goal is to demonstrate that the presence of metals is the main culprit where the Balmer-line problem is concerned. We shall proceed from the most metal-poor stars, the normal DA white dwarfs, and work our way up to the most metal-rich objects, the DAO stars. For each group of stars, we will examine a set of seven wavelength intervals that probe well-known metallic absorption lines present in the FUV spectra of many hot white dwarfs. We list in Table 5 the extent of these intervals as well as the central wavelengths[7] for the spectral lines of interest. We wish to also point out a few particularities in the *FUSE* data. First, there is a very deep absorption feature seen near ∼923 Å, which is ubiquitous in the spectra. This absorption feature is of interstellar origin and is due to neutral hydrogen. Second, many of the lines appear shifted with respect to the central wavelengths indicated by the dotted lines in the figures. These shifts are due to the stellar radial velocity and actually help to distinguish the photospheric lines from interstellar lines.

[7] Taken from the NIST Web site, http://physics.nist.gov/PhysRefData/ASD/lines_form.html.

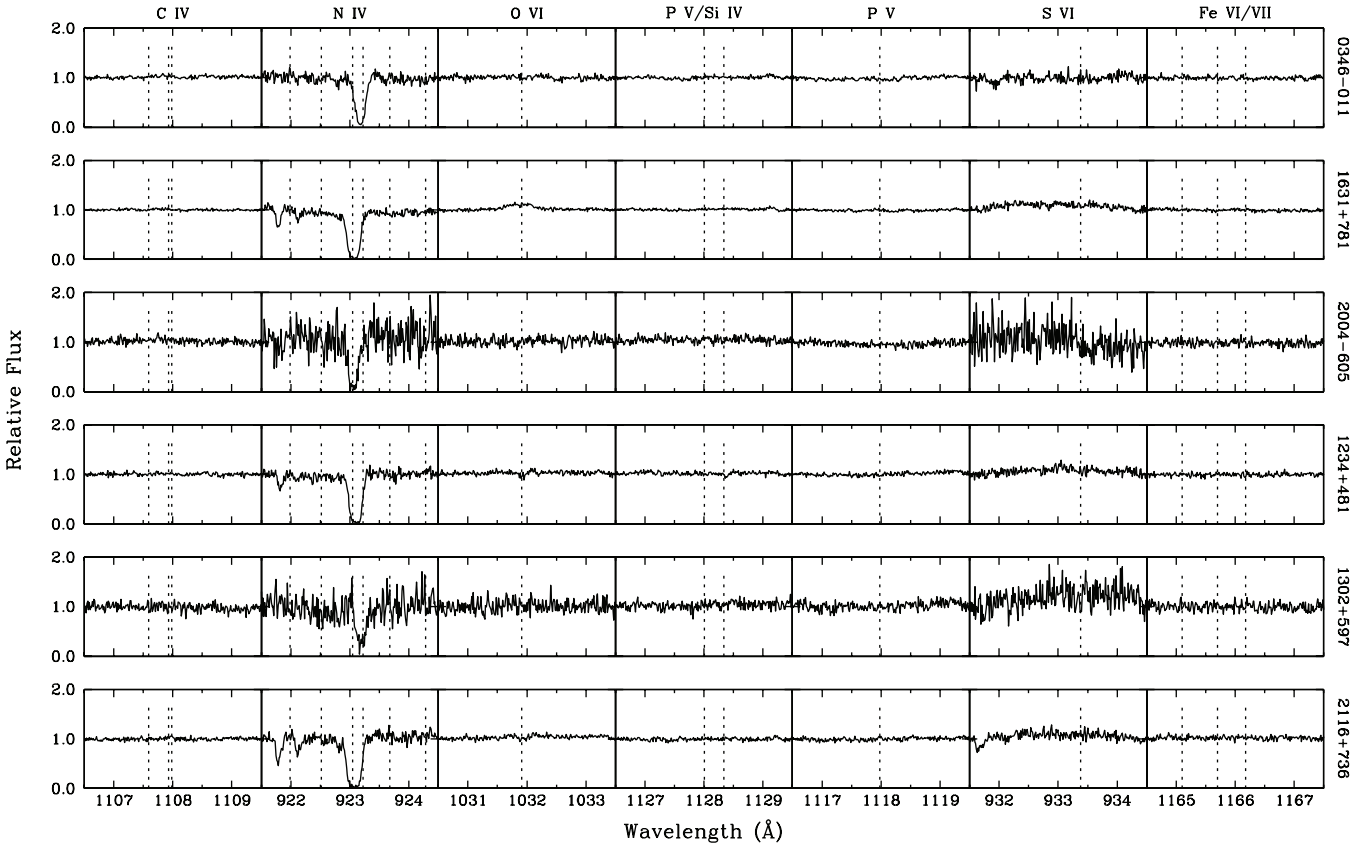

Figure 16. Selected regions of the *FUSE* spectra for six normal DA white dwarfs. Each segment has been normalized to a continuum set to unity. The vertical dotted lines correspond to the central wavelengths of selected lines as listed in Table 5.

The first group of stars is shown in Figure 16. These are six normal DA white dwarfs that do not exhibit the Balmer-line problem. The top three stars in the figure are somewhat cooler with $T_{\rm eff} \sim 45{,}000$ K, whereas the bottom three have $T_{\rm eff}$ in the range 50,000 K $< T_{\rm eff} <$ 60,000 K. With the exception of a few weak N IV lines in some cases, no other metal lines are observed in any of these stars. In particular, 0346−011, one of the coolest objects in Figure 16, is also quite massive with $\log g = 9.13$ and $M = 1.27\ M_{\odot}$; in fact it is the most massive white dwarf seen in Figure 14. This combination of age and high mass has clearly contributed here to produce an FUV spectrum completely devoid of any metal lines. Indeed, any metals in this star likely diffused out of the atmosphere of this star a long time ago and rather quickly at that. These six stars clearly represent the template for metal-poor DA white dwarfs, and consequently they do not suffer from the Balmer-line problem.

Next, we see in Figure 17 examples of hot DA white dwarfs where at least some metal lines are present, particularly the P V/Si IV doublet as well as the P V line near 1118 Å. However, like the stars displayed in Figure 16, they are not afflicted by the Balmer-line problem. In addition, all these stars have $T_{\rm eff}$ in the range 55,000 K $\lesssim T_{\rm eff} \lesssim$ 65,000 K and thus overlap with the bottom three stars of Figure 16 in the $T_{\rm eff}$–log g plane. Since we find stars with and without metals occupying the same range of atmospheric parameters, we must conclude that the presence of metals itself is not only a function of $T_{\rm eff}$ or log g but must also be related to the evolutionary history of each individual object. Of note here is G191-B2B (0501+527), as one of the brightest known white dwarfs ($V = 11.78$) it is consequently one of the most studied white dwarfs as well (Barstow et al. 2001b; Vennes & Lanz 2001; Holberg et al. 2002), and a well-known photometric standard for both ground- and space-based observations (Massey et al. 1988; Turnshek et al. 1990). We see in Figure 17, however, that in the present context G191-B2B does not really stand out and seems to be rather typical of these hot DA white dwarfs that contain some metals, yet do no exhibit the Balmer-line problem.

We now move to Figure 18 where we look at six DA+BP stars. We first note that, in addition to the metal lines observed in the previous group, we see here the appearance, in particular, of O VI and S VI lines, but no iron lines are observed, as in the two previous cases. Some might suggest that these lines are interstellar in origin. However, the strength of the lines and the fact that they are shifted in the same way as the rest of the observed lines in the spectrum strongly suggest they are truly photospheric in nature. The stars in the top three panels have 60,000 K $< T_{\rm eff} <$ 80,000 K but more importantly, they span a large range in surface gravity, from $\log g = 7.13$ for 0621−376 to $\log g = 8.04$ for 1738+669, yet the spectra of all three stars are quite similar. Furthermore, as we can see in Figure 11, the Balmer-line problem is fairly obvious in these three white dwarfs. This once again seems to support our earlier assertion that the presence, or lack thereof, of metals is not only a function of the atmospheric parameters of a star. 0948+534 is the hottest DA+BP in our sample and we see that some of its metallic lines are weaker (P V/Si IV and P V), yet it also shows the strongest O VI lines of these three stars. The higher effective temperature ($T_{\rm eff} \sim 140{,}000$ K) likely induces a different ionization balance that favors O VI but depletes the abundance of the other ions. 0948+534 is also somewhat more massive with $M = 0.67\ M_{\odot}$,

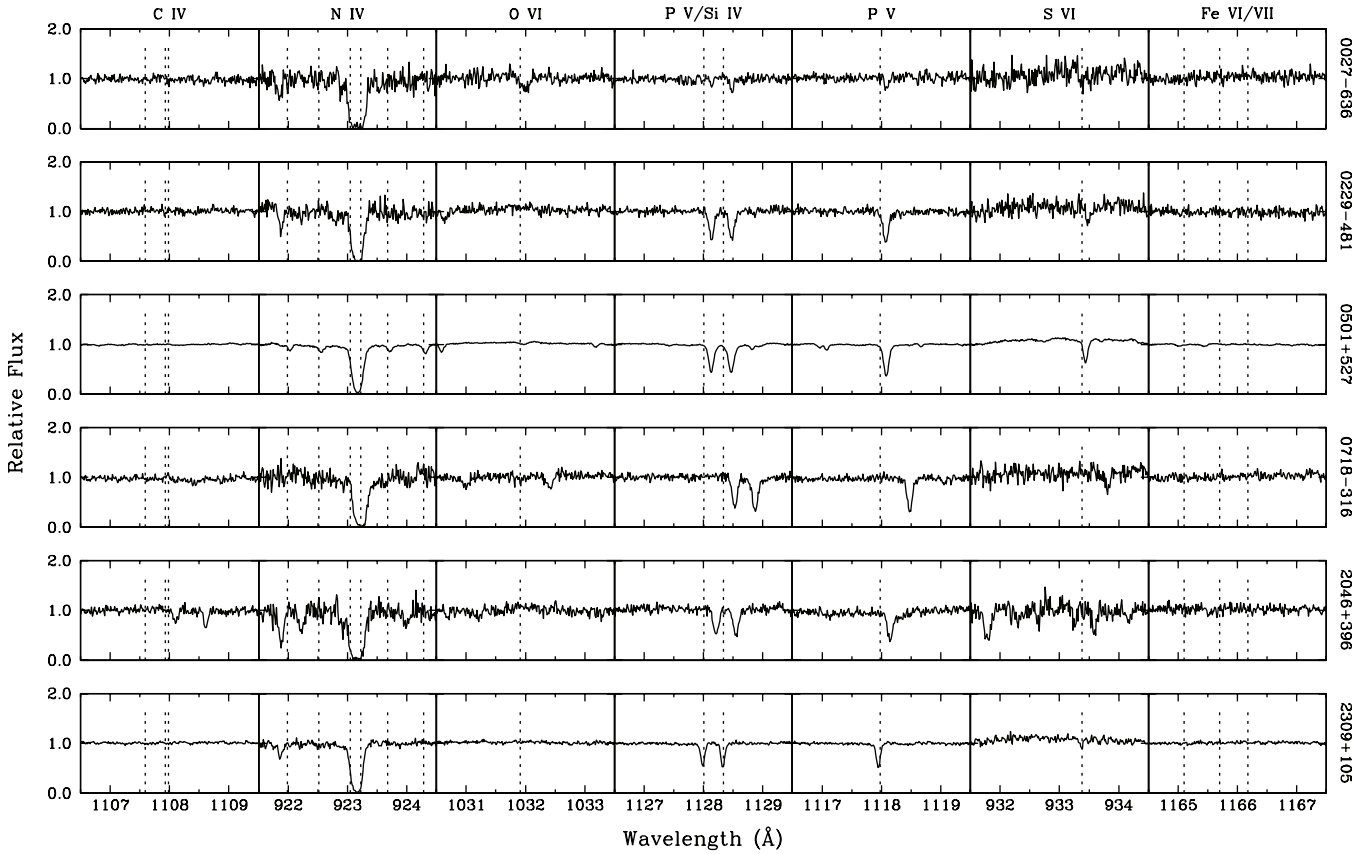

Figure 17. Same as Figure 16 but for six normal DA white dwarfs with some metals.

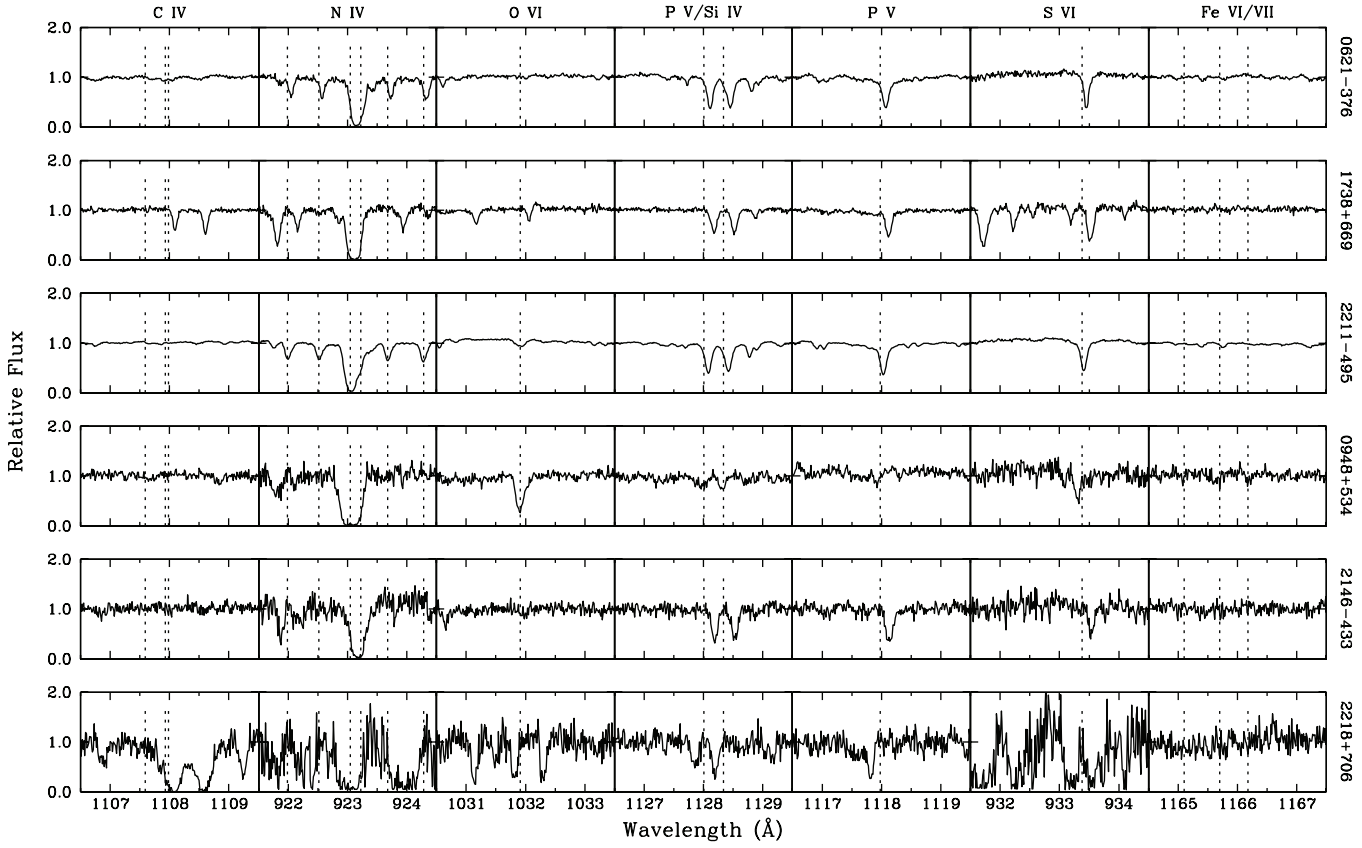

Figure 18. Same as Figure 16 but for six DA white dwarfs exhibiting the Balmer-line problem.

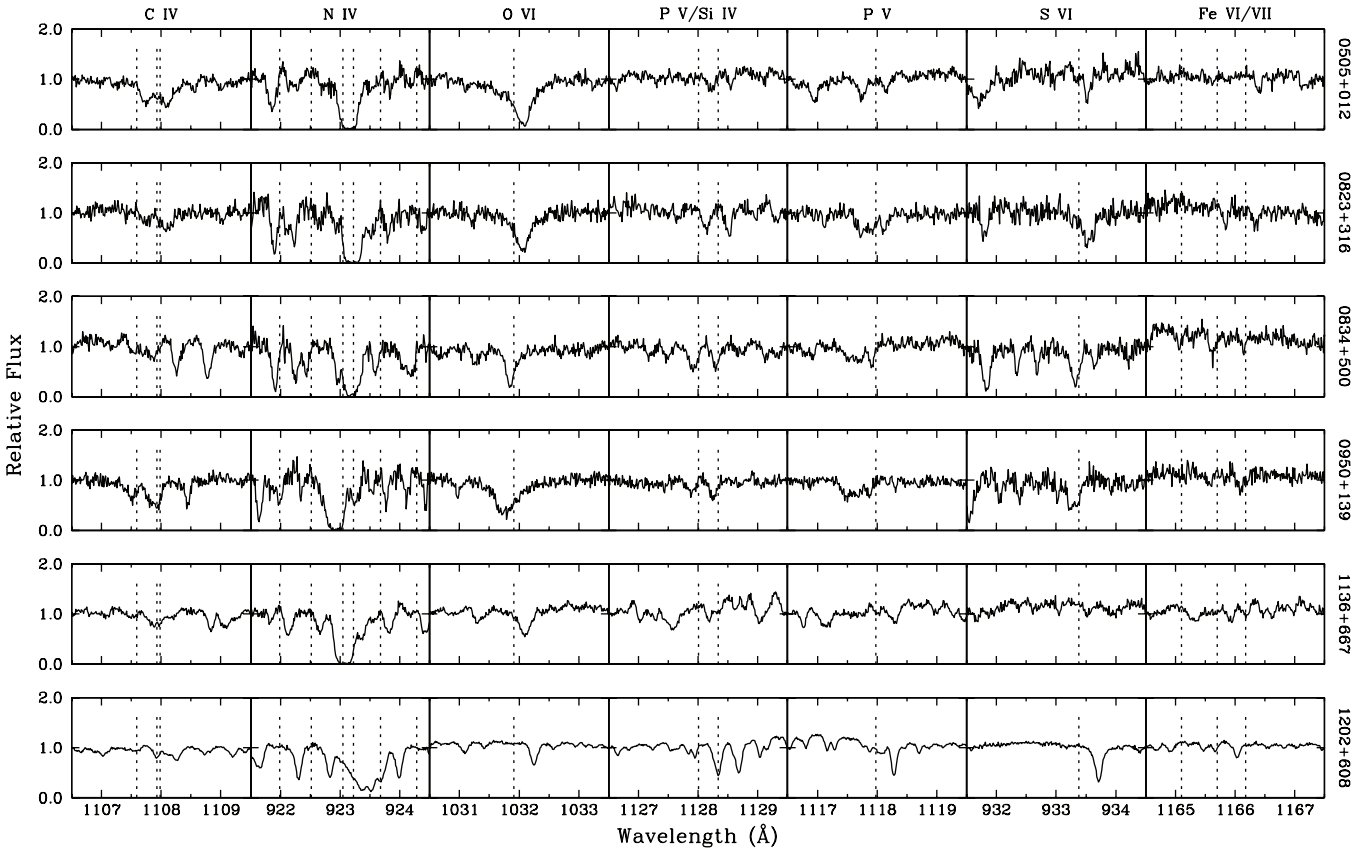

Figure 19. Same as Figure 16 but for six DAO white dwarfs exhibiting the Balmer-line problem.

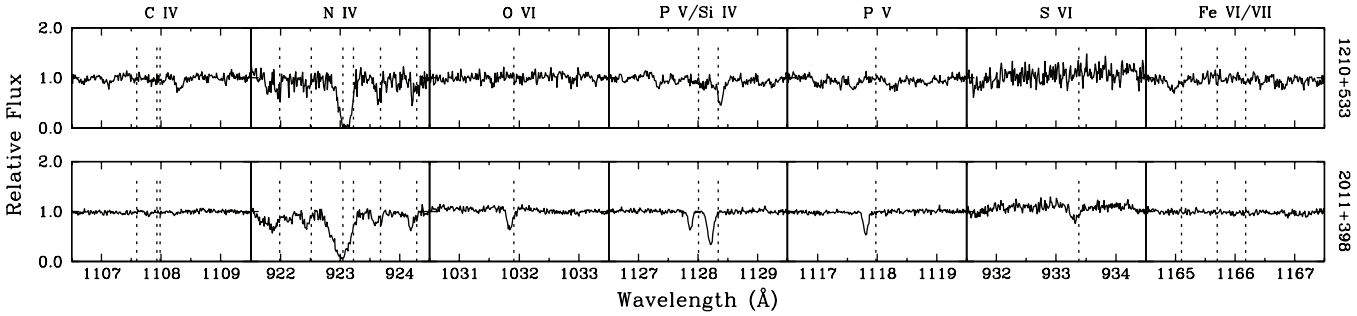

Figure 20. Same as Figure 16 but for two peculiar DAO white dwarfs.

and the Balmer-line problem is not quite as severe in this case. Finally, the spectrum of 2218+706 shows some very deep and wide absorption features which are due to a rather high column density of molecular hydrogen.

We have now arrived at the DAO white dwarfs, which are plotted in Figure 19. We see here a large number of metallic lines in each of the individual wavelength intervals we have chosen, and we finally see the appearance of iron lines. This is in stark contrast to the normal DA white dwarfs we saw in Figures 16–18. DAO white dwarfs are thus clearly the most metal-rich group of stars in our sample and it is not surprising that all the hot DAO stars suffer from the Balmer-line problem. There was, however, one slight exception: 0950+139. As we discussed earlier, the optical spectrum of this star prevents us from determining whether it suffers from the Balmer-line problem. However, its atmospheric parameters are consistent with the bulk of the hotter DAO stars and on that basis we chose to use our CNO grid to fit 0950+139. We see in Figure 19 that it does indeed resemble all the other DAO stars in terms of the presence of metals, thus supporting our earlier decision. Finally, in Figure 20 we show *FUSE* data for two particular DAO white dwarfs. 1210+533 is the DAO white dwarf that Bergeron et al. (1994) had discussed as being spectroscopically variable whereas 2011+398 is one of the three DAO white dwarfs in a DA+dM binary system and does not show the Balmer-line problem. These two stars do not show nearly as many metallic lines as the other DAO stars in Figure 19. Indeed, these two objects are more akin to the DA stars in Figure 17. As such, the fact that 2011+398 contains less metals and does not show the Balmer-line problem is perfectly consistent with the trend we have observed thus far. As for 1210+533, it also seems to be rather metal poor. In this case, the presence of the Balmer-line problem is likely related to its spectroscopic variability than to the presence of metals in the atmosphere.

In summary, we see that, with a few exceptions, the stars in our sample can essentially be divided into four categories in

terms of the presence of metals and the Balmer-line problem. First, there are DA white dwarfs almost completely devoid of metals that do not suffer from the Balmer-line problem, and DA white dwarfs that contain some metals, but do not suffer the Balmer-line problem either. On the other hand, there are DA stars that seem to be quite rich in metals and are afflicted by the Balmer-line problem. Finally, we have the hot DAO white dwarfs that all seem to contain important quantities of metals and consequently all exhibit the Balmer-line problem. It should be clear by now that there is a direct correlation between the presence of metals in the atmospheres of hot white dwarfs and instances of the Balmer-line problem.

6. DISCUSSION

Our analysis of DAO and hot DA white dwarfs has led to some interesting results that have a direct bearing on how we interpret the origin and evolution of these stars. The stars studied in this work represent the largest sample of DAO white dwarfs analyzed in a homogeneous fashion with appropriate model atmospheres. However, one important caveat to keep in mind is that our results would most certainly change if we had precise determinations for the metal abundances in each star. Nonetheless, the new atmospheric parameters, obtained with our improved CNO grid, imply that DAO white dwarfs are hotter, and more massive than previous studies have shown. As a result, we can conclude that most DAO stars are indeed products of post-AGB evolution just like the vast majority of white dwarfs. This is further supported by the knowledge that several of the DAO stars in our sample are CSPN. Indeed, the suggestion by Bergeron et al. (1994) that DAO stars required post-EHB evolution, due to their previously determined lower masses, is no longer valid. We have clearly shown that DAO stars follow the same evolutionary path as the rest of the hydrogen-rich white dwarfs.

This connection is further supported by our discovery that several hot DA stars also suffer from the Balmer-line problem just like DAO stars. In both cases, we used FUV spectra from *FUSE* to demonstrate rather convincingly that the presence of metals is clearly the source of the Balmer-line problem. The only thing that seems to distinguish the DAO stars from their DA counterparts is the presence of helium. As previously discussed, stratified atmospheres and radiative levitation are not able to explain the presence of helium in the atmosphere of these white dwarfs. The most probable cause, as suggested by Bergeron et al. (1994), must therefore be the presence of a weak stellar wind. In that context, the work presented in Unglaub & Bues (2000) is of particular interest here. Although many of their results do not, in a quantitative sense, agree with our own, qualitatively at least, much of what is presented and discussed in Unglaub & Bues (2000) seems to match our results.

The calculations of Unglaub & Bues show that a stellar wind, driven by the presence of metals, can support sufficient amounts of helium in the atmospheres of a white dwarf to explain the observed abundances in DAO stars. However, this is only true up to a limiting temperature known as the "wind limit." Beyond the wind limit, mass loss ceases and heavier elements begin to sink under the influence of gravitational settling. More importantly, Unglaub & Bues showed that when the wind limit is reached, helium sinks more rapidly than CNO. This would allow for a transition region where stars would still have some metals in their atmospheres but no helium. The one major discrepancy between the results of Unglaub & Bues and ours is that their wind limit for DAO stars is ~80,000 K whereas we find several DAOs in the range 60,000 K $< T_{\rm eff} <$ 80,000 K. Otherwise, one

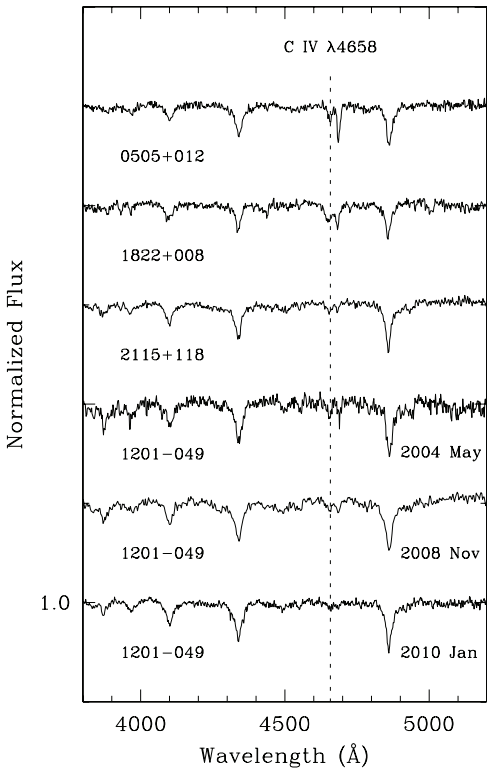

Figure 21. Optical spectra of the four DAOZ white dwarfs in our sample. The bottom three spectra correspond to observations of 1201−049 taken in 2004 May, 2008 November, and 2010 January.

can imagine a scenario whereby DAOs are stars with a wind, driven by metals, that maintains helium in the atmosphere. At the same time, these same metals are also the driving force behind the Balmer-line problem. If the star does not have sufficient helium left, we see it as a DA+BP star instead. On a star-by-star basis, the distinction between a DAO and a DA+BP star would stem from the evolutionary history of each individual object and the initial abundances of helium and metals upon the formation of the white dwarf.

Furthermore, in the presence of mass loss, stratified atmospheres cannot exist because diffusive equilibrium cannot be reached. This would explain why PG 1305−017 is the only DAO white dwarf with a stratified atmosphere as it is cooler than the predicted wind limit. Other stars that are below the wind limit are the three DA+dM systems, this scenario would not apply to them as the DAO nature of these stars most probably stems from interactions with their companion and not from a wind driven by the presence of metals which maintains helium in the atmosphere.

6.1. DAOZ

We show in Figure 21 the four DAOZ white dwarfs in our sample. However, as we alluded to in Section 2, these objects have also been classified as hybrid PG 1159 stars. The first of these objects was uncovered by Napiwotzki & Schönberner (1991). The designation derives from the similarity of their spectra with those of the normal PG 1159 stars, particularly the combination of the He II λ4686 and C IV λ4658 lines. The "hybrid" nature refers to the presence of hydrogen, as evidenced by the strong Balmer lines observed in their spectra. Of particular interest to us is the statement by Dreizler et al. (1995b) that with sufficient hydrogen left in the atmosphere, a

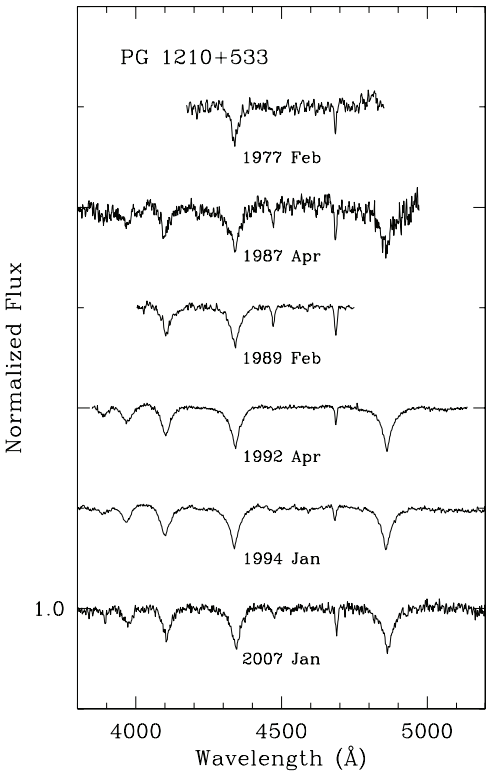

Figure 22. Comparison of our spectrum of PG 1210+533 (1994 January) with spectra obtained over the course of 30 years by Wesemael et al. (1985, 1977 February), Holberg (1987, 1987 April), Kidder (1991, 1989 February), Bergeron et al. (1994, 1992 April), and A. Gianninas (unpublished, 2007 January).

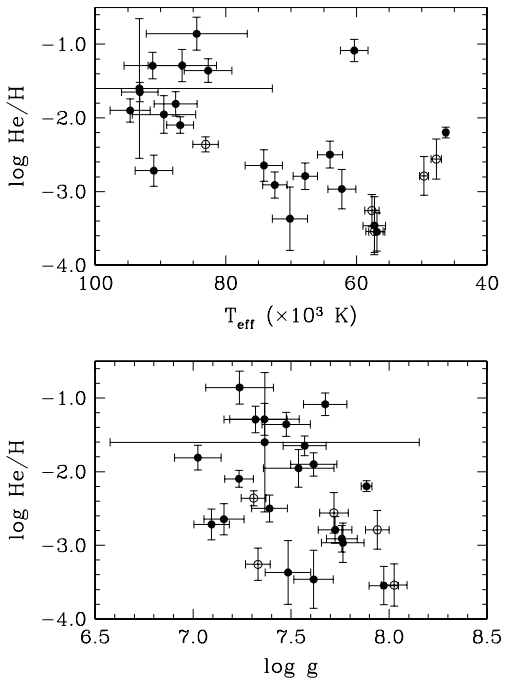

Figure 23. Correlations between the atmospheric parameters of DAO stars (excluding PG 1305−017). DAO stars that are in binary systems are denoted by open circles.

PG 1159 star could become a DA (or DAO) white dwarf once all the metals have diffused out of the atmosphere. The three spectra at the bottom of Figure 21 are all of 1201−049 and span a timescale of almost six years. Specifically, there seems to be an important decrease in the strength of He II λ4686 and C IV λ4658 from the oldest to the most recent observation. It is possible we are witnessing the effects of the metals diffusing out of the atmosphere and this star will eventually present itself as a simple DA or DAO star. Thus, these DAOZ white dwarfs probably represent the transition phase between PG 1159 stars and hot hydrogen-rich white dwarfs corroborating, to a certain extent, the ideas of Fontaine & Wesemael (1987).

6.2. PG 1210+533

One of the unique DAO stars discussed in Bergeron et al. (1994) is PG 1210+553. However, one of the mysteries associated with this object has been solved. We showed in Section 4.2 that the inability of Bergeron et al. (1994) to properly fit the He II λ4686 line profile was a consequence of the one remaining enigma presented by PG 1210+533: its spectroscopic variability. Bergeron et al. (1994) had suggested that further monitoring of this star was necessary in order to decipher its true nature. Since then, two new optical spectra have been obtained: in 1994 January (see Section 2 and Figure 1) and more recently in 2007 January at the Observatoire du Mont-Mégantic with the instrument and setup described in Section 2. We compare in Figure 22 these two spectra with the four spectra shown in Bergeron et al. (1994, see their Figure 16) which were obtained by Wesemael et al. (1985, 1977 February), Holberg (1987, 1987 April), Kidder (1991, 1989 February), and Bergeron et al. (1994, 1992 April). The same type of variability as reported by Bergeron et al. (1994) is observed even in the most recent observations; specifically, the variable strength of He II λ4686 and the appearance and disappearance of He I λ4471, which has re-appeared in the most recent spectrum. We are at odds to explain this strange behavior. Perhaps PG 1210+533 is a hotter counterpart of GD 323, a spectroscopically variable DAB white dwarf (Pereira et al. 2005). In the case of GD 323, Pereira et al. (2005) surmised that the likely causes of the observed variability are inhomogeneities in the surface abundance of helium either as spots, or equatorial belts and polar caps. Similarly, Bergeron et al. (1994) drew comparisons to Feige 7 (Achilleos et al. 1992), a magnetic white dwarf where the spectroscopic variability was interpreted as the surface abundance inhomogeneities of a rotating white dwarf. However, another scenario might also be plausible. Within the paradigm of mass loss as the driving force behind the DAO phenomenon, we established that the stratified nature of PG 1305−017 follows from the extinguishing of the stellar wind which then allows diffusive equilibrium to set in. PG 1210+533 is only ≈2000 K hotter than PG 1305−017. Perhaps we are witnessing a star in the process of establishing that diffusive equilibrium but has not quite gotten there yet. Whatever the case may be, the one certainty is that yet further study is required before the true nature of PG 1210+533 is fully understood.

6.3. Correlations

We plot in Figure 23 the relations between the measured helium abundances of our DAO white dwarfs with respect to $T_{\rm eff}$ and $\log g$. All the values are taken from Table 2. It should be noted that PG 1305−017 is not included in this figure since we have no measurement for the helium abundance in that star. Unlike Bergeron et al. (1994) we do not observe any correlation, in the bottom panel, between $\log g$ and the helium abundance. We do note, however, that the three most massive stars near $\log g \sim 8.0$ all have rather low helium abundances, two of

these being DA+dM binaries (1013−050 and 2011+398). More striking is the rather clear correlation between the helium abundance and $T_{\rm eff}$ seen in the top panel of Figure 23. If the mass-loss scenario we have described above holds, then this is yet another indication of how the weakening stellar wind can no longer maintain helium in the atmosphere of the white dwarf. The three coolest stars in this panel consist once again of two DA+dM binaries (1413+015 and 2011+398) along with PG 1210+533. That the helium abundances in the DA+dM binaries do not match the observed trend is not surprising since the helium in their atmospheres likely results from their binary evolution. Similarly, the fact that PG 1210+533 does not conform to the observed trend is not surprising considering the variable nature of this star and, specifically, of its helium abundance. The DAO star near $T_{\rm eff} \sim 60{,}000$ and log He/H ~ -1.0 is 0505+012, one of the four DAOZ white dwarfs in our sample.

Finally, the object with the very large error bars is 0950+139. The optical spectrum of this star was contaminated with many emission lines from its planetary nebula. All the affected regions, including the core of virtually all the Balmer lines, were necessarily excluded from the fitting procedure thus greatly increasing the uncertainty in the measured atmospheric parameters.

7. CONCLUSION

We have presented a spectroscopic analysis of hot DA and DAO white dwarfs. First, we presented our new grids of NLTE model atmospheres that include CNO to overcome the Balmer-line problem, as prescribed by Werner (1996). By coupling these new models with our standard spectroscopic technique, we were then able to revise the atmospheric parameters of these stars. Our results show that DAO white dwarfs are hotter and more massive as compared to previous determinations. This leads us to the conclusion that DAO white dwarfs are products of post-AGB evolution, not post-EHB evolution as Bergeron et al. (1994) had suggested. Our analysis also uncovered an important number of DA+BP white dwarfs which we analyzed with analogous models. We then employed spectra taken from the *FUSE* archive to show that the presence of metals in both DAO and DA+BP stars are at the origin of the Balmer-line problem.

Clearly, DAO stars form a rather mixed bag of objects. Most of them are products of post-AGB evolution, including many CSPN, and owe their helium to a metal-driven stellar wind. On the other hand, there are also three DA+dM binary systems where the DAO nature is a consequence of interactions with their companion, either through mass exchange or a common envelope phase. Also, we have the two special cases of PG 1305−017 and PG 1210+533. PG 1305−017 is the sole DAO white dwarf that requires a stratified atmosphere. However, even this case can be explained by the mass-loss paradigm because the star is cool enough that mass loss would have ceased, allowing for diffusive equilibrium to be established. On the other hand, PG 1210+533 and its spectroscopic variability still defy explanation.

In the future it would be interesting to see the models of Unglaub & Bues (2000) revisited with new and improved calculations of the mass-loss rates for these stars. In particular, obtaining a better match for the location of the "wind limit" would further cement the case for mass loss as the driving force behind the DAO phenomenon. Additionally, further analyses of the FUSE spectra would be in order to precisely determine, in an absolute manner, the abundances of all metals that are present. This would allow for the calculation of models tailor-made for each object and thus permit the most precise determination of the atmospheric parameters for each star. Finally, as PG 1210+533 still remains a mystery, further monitoring of this object would be warranted if we are ever to truly understand the particular nature of this object.

We thank the director and staff of Steward Observatory and of the Carnegie Observatories for the use of their facilities. We also thank I. Hubeny for his help with the TLUSTY and SYNSPEC packages, P. Dufour for obtaining the spectrum of 0950+139, J. B. Holberg for providing us with his spectrum of HS 1136+6646, and G. Fontaine for useful discussions. Some of the data presented in this paper were obtained from the Multimission Archive at the Space Telescope Science Institute (MAST). STScI is operated by the Association of Universities for Research in Astronomy, Inc., under NASA contract NAS5-26555. Support for MAST for non-HST data is provided by the NASA Office of Space Science via grant NAG5-7584 and by other grants and contracts. This work was supported in part by the NSERC Canada and by the Fund FQRNT (Québec). M.T.R. acknowledges support from FONDAP (15010003) and Proyecto BASAL PB06 (CATA). P.B. is a Cottrell Scholar of Research Corporation for Science Advancement.

REFERENCES

Achilleos, N., Wickramasinghe, D. T., Liebert, J., Saffer, R. A., & Grauer, A. D. 1992, ApJ, 396, 273
Asplund, M., Grevesse, N., & Sauval, A. J. 2005, in ASP Conf. Ser. 336, Cosmic Abundances as Records of Stellar Evolution and Nucleosynthesis, ed. T. G. Barnes III & F. N. Bash (San Francisco, CA: ASP), 25
Barstow, M. A. 1989, in IAU Colloq. 114, White Dwarfs, ed. G. Wegner (New York: Springer), 156
Barstow, M. A., Bannister, N. P., Holberg, J. B., Hubeny, I., Bruhweiler, F. C., & Napiwotzki, R. 2001a, MNRAS, 325, 1149
Barstow, M. A., Burleigh, M. R., Bannister, N. P., Holberg, J. B., Hubeny, I., Bruhweiler, F. C., & Napiwotzki, R. 2001b, in ASP Conf. Ser 226, 12th European Workshop on White Dwarfs, ed. J. L. Provencal et al. (San Francisco, CA: ASP), 128
Barstow, M. A., Dobbie, P. D., Holberg, J. B., Hubeny, I., & Lanz, T. 1997, MNRAS, 286, 58
Barstow, M. A., Good, S. A., Holberg, J. B., Hubeny, I., Bannister, N. P., Bruhweiler, F. C., Burleigh, M. R., & Napiwotzki, R. 2003, MNRAS, 341, 870
Barstow, M. A., et al. 1993, MNRAS, 264, 16
Barstow, M. A., et al. 1995, MNRAS, 272, 531
Bergeron, P., Saffer, R. A., & Liebert, J. 1992, ApJ, 394, 228
Bergeron, P., Wesemael, F., Beauchamp, A., Wood, M. A., Lamontagne, R., Fontaine, G., & Liebert, J. 1994, ApJ, 432, 305
Bergeron, P., Wesemael, F., Lamontagne, R., & Chayer, P. 1993, ApJ, 407, L85
Dixon, W. V., et al. 2007, PASP, 119, 527
Dorman, B., Rood, R. T., & O'Connell, R. W. 1993, ApJ, 419, 596
Dreizler, S., Heber, U., Napiwotzki, R., & Hagen, H.-J. 1995a, A&A, 303, L53
Dreizler, S., Werner, K., & Heber, U. 1995b, in White Dwarfs, ed. D. Koester & K. Werner (Lect. Notes Phys., Vol. 443; Berlin: Springer), 160
Dreizler, S., & Wolff, B. 1999, A&A, 348, 189
Eisenstein, D. J., et al. 2006, ApJS, 167, 40
Fontaine, G., & Wesemael, F. 1987, in IAU Colloq. 95, The Second Conference on Faint Blue Stars, ed. A. G. D. Philip, D. S. Hayes, & J. Liebert (Schenectady, NY: Davis), 319
Fulbright, M. S., Liebert, J., Bergeron, P., & Green, R. 1993, ApJ, 406, 240
Gianninas, A., Bergeron, P., & Fontaine, G. 2005, ApJ, 631, 1100
Gianninas, A., Bergeron, P., & Ruiz, M. T. 2009, J. Phys. Conf. Ser., 172, 012021
Good, S. A., Barstow, M. A., Burleigh, M. R., Dobbie, P. R., Holberg, J. B., & Hubeny, I. 2005a, MNRAS, 363, 183
Good, S. A., Barstow, M. A., Burleigh, M. R., Dobbie, P. R., Holberg, J. B., & Hubeny, I. 2005b, MNRAS, 364, 1082
Good, S. A., Barstow, M. A., Holberg, J. B., Sing, D. K., Burleigh, M. R., & Dobbie, P. D. 2004, MNRAS, 355, 1031

Green, R. F., Schmidt, M., & Liebert, J. 1986, ApJS, 61, 305
Greenstein, J. L. 1984, ApJ, 276, 602
Heber, U., Dreizler, S., & Hagen, H.-J. 1996, A&A, 311, L17
Holberg, J. B. 1987, in IAU Colloq. 95, The Second Conference on Faint Blue Stars, ed. A. G. D. Philip, D. S. Hayes, & J. Liebert (Schenectady, NY: Davis), 285
Holberg, J. B., Barstow, M. A., Hubeny, I., Sahu, M. S., Bruhweiler, F.C., & Landsman, W. B. 2002, BAAS, 34, 765
Holberg, J. B., & Bergeron, P. 2006, AJ, 132, 1221
Holberg, J. B., Kidder, K., Liebert, J., & Wesemael, F. 1989, in IAU Colloq. 114, White Dwarfs, ed. G. Wegner (New York: Springer), 188
Holberg, J. B., Saffer, R. A., Tweedy, R. W., & Barstow, M. A. 1995, ApJ, 452, L133
Homeier, D., Koester, D., Hagen, H.-J., Jordan, S., Heber, U., Engels, D., Reimers, D., & Dreizler, S. 1998, A&A, 338, 563
Hubeny, I., & Lanz, T. 1995, ApJ, 439, 875
Hügelmeyer, S., Dreizler, S., Rauch, T., & Krzesiński, J. 2007, in ASP Conf. Ser. 372, 15th European Workshop on White Dwarfs, ed. R. Napiwotzki & M. R. Burleigh (San Francisco, CA: ASP), 187
Kidder, K. M. 1991, PhD thesis, Univ. Arizona
Kidder, K. M., Holberg, J. B., & Mason, P. A. 1991, AJ, 101, 579
Koester, D. 1989, ApJ, 342, 999
Lamontagne, R., Wesemael, F., Bergeron, P., Liebert, J., Fulbright, M. S., & Green, R. F 1993, in White Dwarfs: Advances in Observation and Theory, ed. M. A. Barstow (Dordrecht: Kluwer), 347
Lemke, M. 1997, A&AS, 122, 285
Liebert, J., Bergeron, P., & Holberg, J. B. 2005, ApJS, 156, 47
Liebert, J., Bergeron, P., & Tweedy, R. W. 1994, ApJ, 424, 817
Liebert, J., Green, R., Bond, H. E., Holberg, J. B., Wesemael, F., Fleming, T. A., & Kidder, K. 1989, ApJ, 346, 251
Massey, P., Strobel, K., Barnes, J. V., & Anderson, E. 1988, ApJ, 328, 315
McCook, G. P., & Sion, E. M. 1999, ApJS, 121, 1
Moos, H. W., et al. 2000, ApJ, 538, L1
Moos, H. W., et al. 2002, ApJS, 140, 3
Napiwotzki, R. 1992, in The Atmospheres of Early-Type Stars, ed. U. Heber & C. S. Jeffery (Berlin: Springer), 310
Napiwotzki, R. 1993, Acta Astron., 43, 343
Napiwotzki, R. 1995, in White Dwarfs, ed. D. Koester & K. Werner (Lect. Notes Phys., Vol. 443; Berlin: Springer), 176
Napiwotzki, R. 1997, A&A, 322, 256
Napiwotzki, R. 1999, A&A, 350, 101
Napiwotzki, R., Green, P. J., & Saffer, R. A. 1999, ApJ, 517, 399
Napiwotzki, R., & Rauch, T. 1994, A&A, 285, 603
Napiwotzki, R., & Schönberner, D. 1991, A&A, 249, L16
Napiwotzki, R., & Schönberner, D. 1993, in IAU Symp. 155, Planetary Nebulae, ed. R. Weinberger & A. Acker (Dordrecht: Kluwer), 495
Napiwotzki, R., & Schönberner, D. 1995, A&A, 301, 545
Pereira, C., Bergeron, P., & Wesemael, F. 2005, ApJ, 623, 1076
Pounds, K. A., et al. 1993, MNRAS, 260, 77
Press, W. H., Flannery, B. P., Teukolsky, S. A., & Vetterling, W. T. 1986, Numerical Recipes (Cambridge: Cambridge Univ. Press)
Saffer, R. A., Livio, M., & Yungelson, L. R. 1998, ApJ, 502, 394
Schöning, T., & Butler, K. 1989, A&AS, 78, 51
Schuh, S. L., Dreizler, S., & Wolff, B. 2002, A&A, 382, 164
Shipman, H. L. 1976, ApJ, 206, L67
Sing, D. K., et al. 2004, AJ, 127, 2936
Tremblay, P.-E., & Bergeron, P. 2009, ApJ, 696, 1755
Turnshek, D. A., Bohlin, R. C., Williamson, R. L., II, Lupie, O. L., Koornneef, J., & Morgan, D. H. 1990, AJ, 99, 1243
Unglaub, K., & Bues, I. 2000, A&A, 359, 1042
Vennes, S. 1999, ApJ, 525, 995
Vennes, S., & Fontaine, G. 1992, ApJ, 401, 288
Vennes, S., & Lanz, T. 2001, ApJ, 553, 399
Vennes, S., Pelletier, C., Fontaine, G., & Wesemael, F. 1988, ApJ, 331, 876
Vennes, S., Thejll, P. A., Galvan, R. G., & Dupuis, J. 1997, ApJ, 480, 714
Werner, K. 1996, ApJ, 457, L39
Werner, K., & Dreizler, S. 1993, Acta Astron., 43, 321
Werner, K., & Heber, U. 1991, in Stellar Atmospheres: Beyond Classical Models, ed. L. Crivellari, I. Hubeny, & D. G. Hummer (Dordrecht: Kluwer), 341
Wesemael, F., Green, R. F., & Liebert, J. 1985, ApJS, 58, 379
Wolff, B., Koester, D., Dreizler, S., & Haas, S. 1998, A&A, 329, 1045
Wood, M. A. 1995, in White Dwarfs, ed. D. Koester & K. Werner (Lect. Notes Phys., Vol. 443; Berlin: Springer), 41